

000 BEYOND ACCURACY: ARE TIME SERIES FOUNDATION 001 MODELS WELL-CALIBRATED? 002

003 **Anonymous authors**
004
005 Paper under double-blind review
006

007 ABSTRACT 008

009 The recent development of foundation models for time series data has generated
010 considerable interest in using such models across a variety of applications. Al-
011 though foundation models achieve state-of-the-art predictive performance, their
012 calibration properties remain relatively underexplored, despite the fact that cali-
013 bration can be critical for many practical applications. In this paper, we investigate
014 the calibration-related properties of five recent time series foundation models and
015 two competitive baselines. We perform a series of systematic evaluations assess-
016 ing model calibration (i.e., over- or under-confidence), effects of varying predic-
017 tion heads, and calibration under long-term autoregressive forecasting. We find
018 that time series foundation models are consistently better calibrated than base-
019 line models and tend not to be either systematically over- or under-confident, in
020 contrast to the overconfidence often seen in other deep learning models.
021

022 1 INTRODUCTION 023

024 Prediction and modeling of time series data is ubiquitous in data analysis, with applications across
025 a broad range of fields including climate science (Mudelsee, 2014), energy forecasting (Deb et al.,
026 2017), healthcare (Crabtree et al., 1990), consumer behavior modeling (Goel et al., 2010), and fi-
027 nancial forecasting (Tsay, 2005). Traditional statistical approaches such as linear autoregressive
028 (AR) models and associated variants are well-established in the field (Hamilton, 1994; Hyndman
029 & Athanasopoulos, 2018); they have been supplemented in recent years by a variety of machine
030 learning approaches using richer model representations, including deep learning time series models
031 such as N-BEATS (Oreshkin et al., 2019) and Informer (Zhou et al., 2021).
032

033 A more recent trend is the emergence of *time series foundation models (TSFMs)* (Nie et al., 2023;
034 Liang et al., 2024). Unlike traditional statistical and machine learning approaches where models
035 are fitted to time series from a single source, TSFMs are general-purpose models trained on a broad
036 range of time series from various domains and are capable of zero-shot or few-shot forecasting on
037 any time series in principle (Ye et al., 2024; Liang et al., 2024). This is appealing to practitioners
038 in that only a single global model is required rather than retraining a new model for every time
039 series (Bommasani et al., 2021; Benidis et al., 2022).
040

041 With this increase of interest in TSFMs, it becomes important to understand and characterize the
042 calibration properties of such models. TSFMs, in general, produce conditional distributions over
043 potential future values, rather than just single point forecasts (e.g., the expected value of the time
044 series at a future time). This distributional information is important and useful in many applications.
045 In particular, it can be essential for decision-making (Gneiting et al., 2007; Petropoulos et al., 2022),
046 for example in downstream tasks such as anomaly detection (Menon & Williamson, 2018) and in
047 critical domains such as healthcare (Farah et al., 2014; Marlin et al., 2012). A natural question in
048 this context is: **how well calibrated are TSFMs in terms of their conditional distributions, i.e.,**
049 **how well do the predicted probabilities match the observed data?**

050 While the calibration properties of classification and regression models have received considerable
051 attention in machine learning in recent years (e.g., Guo et al. (2017); Song et al. (2019); Chung et al.
052 (2021)), the calibration properties of TSFMs remain relatively underexplored. To address this gap,
053 we perform an empirical study of TSFMs and baselines with respect to *calibration-specific metrics*.
Our systematic evaluation includes five state-of-the-art TSFMs and two well-established baseline
methods in terms of their zero-shot forecasts across six univariate time series datasets with different

054 temporal granularities. We measure calibration properties through a comprehensive set of metrics,
 055 such as Probabilistic Calibration Error (Dheur & Taieb, 2023; Kuleshov et al., 2018; Chung et al.,
 056 2021), in the context of a variety of different aspects of conditional uncertainty in model predictions.
 057

058 In general, TSFMs produce conditional distributions using two approaches: some models predict the
 059 parameters of conditional density models (Rasul et al., 2023; Woo et al., 2024; Ansari et al., 2024a),
 060 while others predict sets of conditional quantiles (Das et al., 2024; Auer et al., 2025; Wang et al.,
 061 2025). To fully understand the calibration properties of TSFMs, we isolate the impact of different
 062 prediction heads by training individual quantile and distribution heads for each of the TSFM base
 063 architectures and then evaluate the effect of prediction heads on calibration performance.
 064

065 Additionally, TSFMs vary in their approaches for long-term forecasting. For long-term forecasting
 066 beyond the *forecast horizon* (the prediction length of a single forward-pass), many TSFMs rely
 067 on autoregressive forecasting (Das et al., 2024; Ansari et al., 2024b; Cohen et al., 2025). Prior
 068 works (Auer et al., 2025; Wang et al., 2025) have shown that using autoregressive forecasting can
 069 have negative effects on model performance due to the reinitialization of the probabilistic forecast.
 070 Solutions include multi-patch forecasting (Woo et al., 2024) where models can predict sequential
 071 patches at a time, and stochastic autoregression which propagates probabilistic information to sub-
 072 sequent forecasts as described in Section 3.2. In this context, it is important to understand how lim-
 073 ited forecast horizons can affect calibration on long-term forecasts. To investigate this, we compare
 074 TSFM calibration on long-term forecasting across varying forecast horizon lengths and autoregres-
 075 sive implementations.
 076

077 The primary contributions of our work are as follows:
 078

- 079 • We conduct a first-of-its-kind systematic calibration study with five state-of-the-art founda-
 080 tion models and two well-established baselines across six datasets from different domains¹.
- 081 • We use three calibration-specific metrics to quantify the overall calibration error and over-
 082 and under-confidence of prediction models; we analyze the calibration effects of various
 083 distributional and quantile prediction heads; and we investigate the effect of different long-
 084 range forecasting methods on calibration.
- 085 • We find that TSFMs are better calibrated than baseline models, tend to be neither system-
 086 matically over- nor under-confident, are generally insensitive to the form of distributional
 087 prediction head, and consistently competitive in both prediction and calibration.

088 2 BACKGROUND AND RELATED WORK

089 2.1 PROBABILISTIC TIME SERIES FORECASTING

090 Given a *context* of T observations $y_{1:T}$ for a time series, we evaluate the H -length forecasting
 091 performance on the prediction $y_{T+1:T+H} \mid y_{1:T}$. We denote the median prediction as $\hat{y}_t^{0.5}$ at each
 092 $t \in \{T+1, \dots, T+H\}$ for point estimates, and predicted quantiles \hat{y}_t^q to assess the uncertainty and
 093 calibration. The predicted quantiles are either produced directly by a multi-quantile prediction head
 094 for each of the H future points, or can be computed from the predicted conditional density.

095 TSFMs can differ slightly in their approaches to data aggregation and functionality, but typically
 096 they tokenize time series in patches of a predetermined length (Nie et al., 2023). We denote the
 097 *forecast horizon* p as the number of future time steps a model can forecast in a single forward-
 098 pass. When the desired forecast length H is greater than the model’s forecast horizon p , a simple
 099 approach is to use autoregressive (AR) forecasting based on point estimates, where the model will
 100 incorporate the previous forecasts $\hat{y}_{T+1:T+p}$ into the observed context. The model then uses this
 101 extended and shifted context $y_{1+p:T+p}$ to forecast the next set of patches $\hat{y}_{T+p+1:T+2p}$, recursively
 102 until the desired forecast $\hat{y}_{T+1:T+H}$ is reached (Ansari et al., 2024b; Cohen et al., 2025). Methods to
 103 reduce the reliance on AR forecasting include extending the number of simultaneous output patches
 104 in multi-patch forecasting (Woo et al., 2024), increasing output patch length (Das et al., 2024),
 105 and incorporating missing-data masks to extend the context into the future (Auer et al., 2025). We
 106 empirically compare these approaches for long-term forecasting in Section 4.4.

107 ¹We will provide the full code base for reproducing our experiments and links to datasets in a GitHub
 108 repository in the final version of our paper.

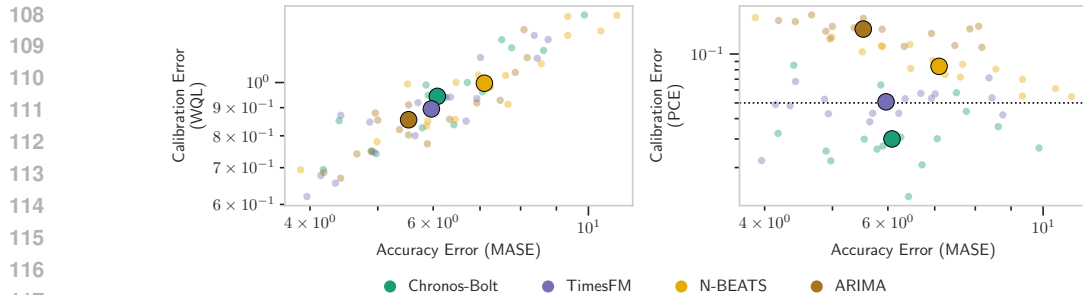


Figure 1: **Weighted Quantile Loss (WQL) calibration metric can be highly correlated with point accuracy error (MASE).** Results shown for WQL (left) and PCE (right) plotted against MASE on the Glucose dataset used in our experiments. Background markers are results for each model and each individual time series; larger centroids are medians across time series. **On this dataset, WQL incorrectly identifies ARIMA as the best calibrated model.**

In TSFMs, patched time series are passed into a model-specific backbone, which translates the embeddings into a latent space as an input to the final projection block. These probabilistic predictions can then be directly predicted as quantiles through a multi-headed projection block or a model can use the latent activations to output the parameters to a distribution where the full densities can be recovered. Some prediction heads can better represent different types of data, for instance negative binomial would be well-suited for count data, while a Student’s t distribution would be appropriate for a general continuous-valued time series. Furthermore, parameterizations of mixture of distributions, as well as quantile heads, have also been proposed (Woo et al., 2024; Das et al., 2024; Cohen et al., 2025) to allow for additional flexibility in terms of how TSFMs can model conditional distributions. We evaluate these different projection blocks across a range of domains to identify if certain heads are better calibrated for specific datasets in Section 4.3.

2.2 RELATED WORK ON CALIBRATION

Predictive calibration has long been recognized as a topic of importance in statistics and machine learning (Brier, 1950; Gneiting et al., 2007). In recent years, a number of different studies have investigated the calibration of deep learning models, and have shown that such models are often systematically susceptible to overconfidence, for example in image classification with deep models (Guo et al., 2017; Ye et al., 2023; Pinto et al., 2022) and in multiple question-answering tasks for large language models (Jiang et al., 2021; Mielke et al., 2022; Xiong et al., 2024).

In the evaluation of time series forecasting models, calibration is also an important component (Makridakis et al., 2022; Aksu et al., 2024; Das et al., 2024). One of the most commonly used calibration metrics is the Continuous Ranked Probability Score (CRPS), which directly compares the cumulative distribution function (CDF) of model predictions to the observed value’s CDF (Hersbach, 2000). Since computing CRPS can be intractable and some TSFMs only produce quantiles rather than full conditional densities, the Weighted Quantile Loss (WQL) is also often used as a discrete surrogate for CRPS (Woo et al., 2024; Aksu et al., 2024), defined as the pinball (or quantile) loss scaled by the absolute sum of the true values. Another common calibration metric is Mean Scaled Interval Score (MSIS) (Makridakis et al., 2020), which takes the mean difference in upper and lower bound predictions and adds an error penalty when the true value lies outside the bounds.

Using these metrics, prior works have claimed that TSFMs are better calibrated than baseline methods like ARIMA and N-BEATS (Aksu et al., 2024; Ansari et al., 2024a; Auer et al., 2025). However, Chung et al. (2021) proved that the metrics above (CRPS, WQL, MSIS) measure a combination of both probabilistic calibration and sharpness (Gneiting et al., 2007), rather than calibration alone. This combination can result in an imbalance in evaluation that can skew towards prioritizing predictive sharpness (Chung et al., 2021). Figure 1 shows a concrete example of how PCE and WQL can differ in practice: WQL can be highly correlated with Mean Absolute Scaled Error (MASE), while PCE directly measures calibration. In the next section, we discuss calibration-focused metrics that address this issue by focusing solely on measuring calibration.

162

3 EXPERIMENTAL SETUP

163

3.1 METRICS

164 The first calibration metric we use is **Probabilistic Calibration Error (PCE)** (Kuleshov et al., 2018;
165 Dheur & Taieb, 2023):

166
$$167 \text{PCE} = \frac{1}{|Q|} \sum_{q \in Q} \left| q - \frac{1}{H} \sum_{t=T+1}^{T+H} \mathbf{1}[y_t \leq \hat{y}_t^q] \right|, \quad (1)$$

168 where $q \in Q = \{0.1, 0.2, \dots, 0.9\}$ is the set of quantiles that we average over in our experiments.
169 Intuitively, PCE measures the differences between empirical and predicted CDFs with lower values
170 indicating better-calibrated models. PCE is lower-bounded by 0 and upper-bounded by 0.5 for the
171 case where predicted quantiles are always all above or below the observed value y_t .172 However, well-calibrated models are not sufficient to produce useful forecasts: a model could for
173 example always predict the marginal distribution, independent of the inputs. In this context, a metric
174 that specifically captures *sharpness* (the concentration of the predictive distributions) is also
175 important in an overall evaluation of calibration (Gneiting et al., 2007; Kuleshov et al., 2018). A
176 simple surrogate for sharpness is the width of a predicted confidence interval, e.g., where an 80%-
177 confidence interval is the interval between the symmetric $q_{\text{low}} = 10\%$ and $q_{\text{high}} = 90\%$ quantile
178 predictions. We refer to this as **Scaled Interval Width (SIW)** where s is the confidence associated
179 with the interval (i.e., $s = q_{\text{high}} - q_{\text{low}} = 80\%$ in the preceding example):
180

181
$$182 \text{SIW}_s = \frac{1}{H} \sum_{t=T+1}^{T+H} \frac{\hat{y}_t^{q_{\text{high}}} - \hat{y}_t^{q_{\text{low}}}}{y^{q_{\text{high}}} - y^{q_{\text{low}}}}. \quad (2)$$

183 Models with lower SIW values (i.e., tighter prediction intervals) are more confident in their predictions,
184 while models with larger SIW values (i.e., wider-spread predictions) are less confident.185 We are also interested in whether a model is systematically miscalibrated in one direction or another. To quantify this, we define the metric **Centered Calibration Error (CCE)** that compares the
186 amount of observed data in a predicted interval with the associated confidence s :

187
$$188 \text{CCE} = \frac{1}{|S|} \sum_{s \in S} s - \frac{1}{H} \sum_{t=T+1}^{T+H} \mathbf{1}[\hat{y}_t^{q_{\text{low}}} \leq y_t \leq \hat{y}_t^{q_{\text{high}}}] \quad (3)$$

189 A model's over- or under-confidence can be identified by combining the direction of CCE and its
190 SIW. Positive CCE values indicate there is more observed data outside the predicted interval than
191 expected by the confidence level; together with a low SIW value, we can infer that a model is
192 overconfident. On the other hand, negative CCE values and larger SIW values imply that the model
193 is under-confident. For both CCE and SIW, we average over $s \in \{0.2, 0.4, 0.6, 0.8\}$ in our analyses.194 Finally, to assess the point accuracy of TSFMs (independently from any calibration error) we use
195 **Mean Absolute Scaled Error (MASE)** for the predicted median, scaling the Mean Absolute Error
196 (MAE) by a naive predictor (Hyndman & Athanasopoulos, 2018):

197
$$198 \text{MASE} = \frac{\frac{1}{H} \sum_{t=T+1}^{T+H} |\hat{y}_t^{0.5} - y_t|}{\frac{1}{H-1} \sum_{t=T+2}^{T+H} |y_t - y_{t-1}|}. \quad (4)$$

199 Note that for multi-step predictions ($H > 1$) that the MAE of the naive predictor in the denominator
200 is in effect using information “from the future,” with the result that the overall MASE may take
201 values greater than 1 even for useful models. The absolute values of MASE are not important, but
202 the relative MASE values across different predictors \hat{y} are what we will focus on.203

3.2 MODELS

204 **Base Models** We evaluate calibration properties of five TSFMs in terms of their zero-shot forecasts:
205 Chronos-Bolt (Ansari et al., 2024a;b), TimesFM (Das et al., 2024), Moirai 2.0 (Woo et al.,
206 2024; Taha Aksu et al., 2025), TiReX (Auer et al., 2025), and YingLong (Wang et al., 2025). As

216 baselines, we use ARIMA (Hyndman & Khandakar, 2008) and N-BEATS (Oreshkin et al., 2019)
 217 to represent well-known parametric and neural time-series prediction alternatives to TSFMs. All
 218 selected TSFMs have been pretrained on various large pretraining datasets and use a quantile pre-
 219 diction head. Additionally, they all use transformers, except for TiRex which uses an xLSTM (Beck
 220 et al., 2024) backbone. TimesFM, Moirai 2.0, and TiRex use a decoder-only architecture with a
 221 causal attention mechanism, while Chronos-Bolt uses the encoder-decoder backbone from the T5
 222 model (Raffel et al., 2020) and YingLong uses a bi-directional encoder-only architecture.

223
 224 **Autoregressive Methods** Autoregressive (AR) forecasting is often necessary for models with a
 225 limited forecast horizon for long-term forecasting. Each model implements AR forecasting slightly
 226 differently. Chronos-Bolt and TimesFM use a naive point-based AR, where only the mean or
 227 median predictions are autoregressively added to the context. This method while simple is known
 228 to significantly harm probabilistic forecasting due to the re-initialization of the context each itera-
 229 tion (Auer et al., 2025). Improvements to the naive method typically require forecasting each time
 230 step multiple times with different AR contexts to propagate probabilistic information across fore-
 231 cast iterations: Moirai 2.0 implements a branching approach which autoregressively forecasts using
 232 a separate context for each quantile. The Toto TSFM (Cohen et al., 2025) uses a trajectory approach
 233 which produces n (usually $\gg |Q|$) independent AR forecasts or trajectories, where each trajectory
 234 is produced similarly to the point-based approach. Instead of adding the mean or median forecast to
 235 the context, it adds a random sample from the predicted distribution at each time step. We explain
 236 these methods in more detail in Appendix A.3. These AR methods trade off robustness for com-
 237 putational efficiency, where the TimesFM and Chronos-Bolt approach only forecasts each time step
 238 once, while the branching (Moirai 2.0) and trajectory approach (Toto) require $|Q|$ and n forecasts
 239 per time step respectively. In addition to comparing these AR methods, we evaluate how larger or
 240 smaller forecast horizons affect calibration on long-term AR forecasting.

241 3.3 DATASETS

242 We selected evaluation datasets representing a range of tasks differing in time-step granularity, sea-
 243 sonality, and forecasting difficulty across a variety of domains. To the best of our knowledge, these
 244 datasets were not used in the training of the foundation models (except the M5 data for the Moirai 2.0
 245 and YingLong models). Each dataset is split into a train and test set where the non-TSFMs, ARIMA
 246 and N-BEATS, are trained independently on the train set, where hyperparameters are chosen by Au-
 247 toARIMA and grid search respectively. All models are evaluated on the held-out test set. Table 1
 248 summarizes the dataset statistics. Our results on each dataset are aggregated over multiple settings
 249 (see Section 3.1), prediction steps, and all possible context-prediction combinations in the test set
 250 for each time series, i.e., effectively generating many more time series forecasts than the number of
 251 time series (see the last column in Table 1). Additional details are provided in Appendix A.2.

252
 253 Table 1: Datasets used in calibration experiments.

	# Time Series	Granularity	Time Steps per Series	# Total Forecasts
Reviews	239	Hourly	13,000	360,490
Shopping (M5)	70	Daily	1,912	62,160
Glucose	16	5 Mins	1,686	13,840
Heart-Rate	6	Second	744	1,800
Crime	5	Daily	6574	4,110
Patents	83	Monthly	408	10,956

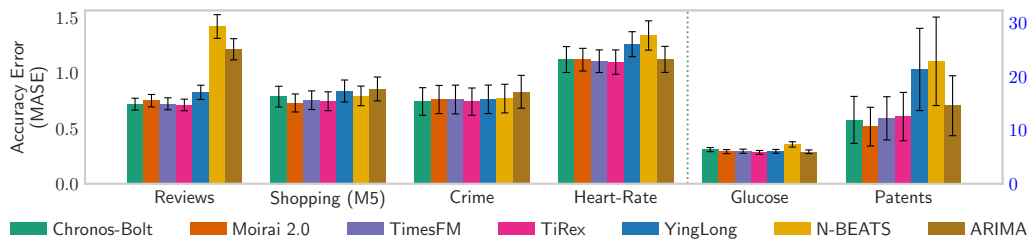
254
 255 To evaluate the effect of different prediction heads for the TSFMs, we trained prediction heads using
 256 a large diverse dataset that is comparable to those used in TSFM pretraining. Specifically, we se-
 257 lected **TSMixup** from Ansari et al. (2024a) as it is independent of the six datasets we use to evaluate
 258 the models. This allows the trained projection blocks to be an equivalent plug-in replacement to the
 259 default quantile projection heads of the selected models.

270

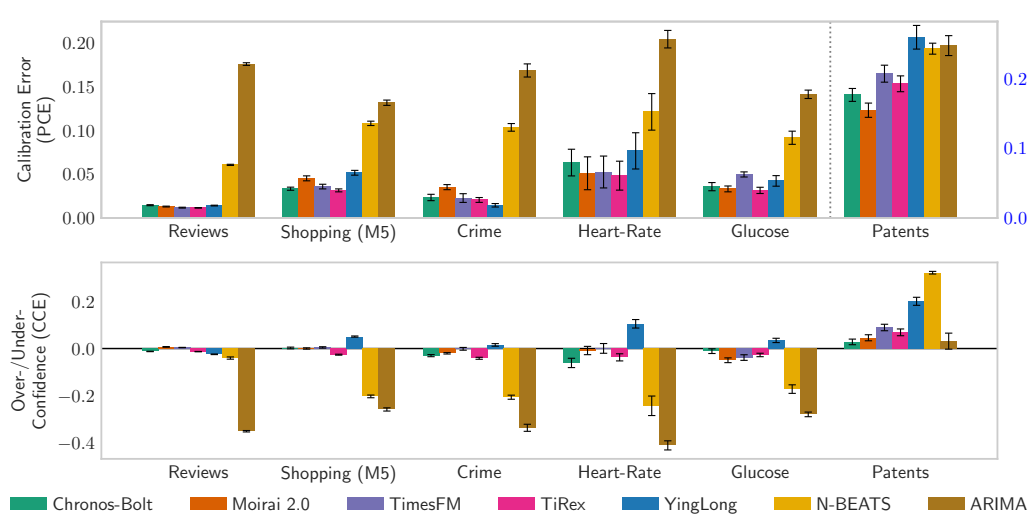
4 EXPERIMENTS

271
 272
 273 Based on the models, datasets, and metrics outlined above, we found that foundation models exhibit
 274 competitive and often better point-forecasting performance compared to baselines, with the TSFMs
 275 often having a lower MASE than N-BEATS and ARIMA (see Figure 2). The Glucose and Patents
 276 datasets have significantly higher MASE numbers than the other datasets—this may be due to the
 277 fact that for each of these datasets there appears to be little significant linear dependence beyond 1
 278 or 2 lags (see partial autocorrelation plots in Figure 6 in Appendix B.4).

279 TSFMs also exhibit significantly better calibration performance than baseline models. We discuss
 280 the main results on calibration in detail below. In the Appendix, we also include additional figures
 281 and findings, where we discuss the empirical correlation of WQL, MSIS, and MASE, along with
 282 details on the calibration of tail probabilities.



293 **Figure 2: TSFMs offer competitive point forecasting performance compared to the baseline**
 294 **models, often having better accuracy than the baselines.** *y*-axis: Mean Absolute Scaled Error
 295 (MASE) measuring point accuracy error of the median prediction (lower is better), Glucose and
 296 Patents use their own *y*-axis scale (on the right). The error bars are computed as the Standard Error
 297 of the Mean (SEM) across timeseries.



300 **Figure 3: TSFMs are better calibrated than the baseline models and are not systematically**
 301 **over- or under-confident.** Top: Probabilistic Calibration Error (PCE) across datasets and models
 302 using the default quantile projection block. (Patents PCE uses its own *y*-axis scale (on the right)).
 303 Lower PCE values are better. Bottom: Centered Calibration Error (CCE) evaluating systematic
 304 overconfidence (positive) or under-confidence (negative).

324 4.1 ARE FOUNDATION MODELS WELL-CALIBRATED?
325

326 Previous works have indicated that TSFMs are well calibrated using CRPS, WQL, and MSIS (Aksu
327 et al., 2024; Auer et al., 2025), but as discussed in Section 3.1 and in Chung et al. (2021), these
328 metrics can be biased towards sharpness and accuracy rather than reflecting calibration per se. In
329 our experiments, we evaluate directly if TSFMs are well-calibrated, focusing on the PCE metric,
330 and we find that, yes, **TSFMs are generally better calibrated than the baseline models of N-**
331 **BEATS and ARIMA**: see top plot in Figure 3. For a general sense of scale, PCE values below
332 0.05 or 5% error relative to the quantiles can loosely be considered to be much better calibrated than
333 values larger than say 0.15, in the context of the range of PCE being between 0 and 0.5. The TSFMs
334 are in general close to or below 5% in PCE error, except for the relatively difficult Patents dataset
335 where all methods (TSFMs and baselines) have high calibration error. No single TSFM significantly
336 dominates in calibration performance over the others.

337 A natural additional question is how calibration performance is affected by how far in time a model
338 prediction is from the context. Naturally, as both TSFMs and baselines predict further into the
339 future, both the point accuracy (MASE) and calibration error (PCE) degrade (see Figures 7 and 8 in
340 the Appendix). However, calibration overall remains relatively stable with TSFMs achieving PCE
341 values close to or below 5% even 64 time-steps out (e.g., for Reviews, M5, and Crime data), unlike
342 the baseline models which have a consistently high PCE over all prediction lengths.

343 As a control experiment, we also evaluated the calibration performance of TSFMs on two synthetic
344 datasets, one with pure IID noise $y_t = \epsilon$ and the other a noisy first-order linear process $y_t =$
345 $\alpha y_{t-1} + (1 - \alpha)\epsilon$, with $\epsilon \sim \mathcal{N}(0, 1)$ and $\alpha = 0.9$. For these datasets the question of interest is
346 whether TSFMs might overfit (for either calibration or point prediction) relative to a baseline like
347 ARIMA (which in principle can be perfect on these datasets). As shown in the lower right two plots
348 in Figure 9 in the Appendix, the TSFMs do not overfit (they perform well on both MASE and PCE).
349 ARIMA does well on MASE but is not as well-calibrated (PCE) (nor is N-BEATS) as the TSFMs.

350 In summary, while past works have shown that TSFMs perform well on WQL and CRPS metrics
351 (e.g., Aksu et al. (2024); Ansari et al. (2024a); Auer et al. (2025)), as we discussed earlier (see Figure
352 1 and further in Appendix B.2), WQL alone is not necessarily a reliable indicator of calibration
353 performance. Our results provide direct confirmation that TSFMs tend to be well-calibrated.

354 4.2 ARE FOUNDATION MODELS SYSTEMATICALLY BIASED IN MISCALIBRATION?
355

356 For image and text modalities, deep models are well-known to often be overconfident (Ye et al.,
357 2023; Xiong et al., 2024; Kapoor et al., 2024). In the context of time series, it is natural to ask if
358 TSFMs similarly exhibit systematic biases, either towards over- or under-confidence.

359 To answer this, we evaluated the CCE metric across datasets and models. The lower plot in Figure 3
360 shows the directionality of model confidence. Except for the Patents dataset, where all models are
361 overconfident, we find that **TSFMs tend not to be systematically over- or under-confident**. In
362 contrast, N-BEATS and ARIMA are consistently under-confident. As shown in Figure 12 in the Ap-
363 pendix, the interval width (SIW) and centered calibration (CCE) tend to have a negative correlation:
364 models with wider confidence intervals tend to have a smaller CCE or are under-confident.

365 It is noteworthy that TSFMs are not systematically overconfident, in the way that foundation models
366 from the text and image domains tend to be. This can likely be explained by the fact that TSFMs are
367 being directly trained with a calibration-aware loss (i.e., trained to minimize WQL), while text and
368 image models are trained to minimize reconstruction or classification error.

369 4.3 HOW DO PREDICTION HEADS AFFECT CALIBRATION?
370

371 A major design choice of TSFMs is selecting a suitable prediction head. Multiple approaches have
372 been presented in the literature, including quantile prediction heads (the default choice for all TSFMs
373 in our experiments), parametric distribution heads (e.g., Lag-Llama (Rasul et al., 2023) with Stu-
374 dent’s t), categorical distribution heads (e.g., Chronos (Ansari et al., 2024a)), and semi-parametric
375 mixture heads such as Toto (Cohen et al., 2025) and Moirai 1.0 (Woo et al., 2024) which use a variety
376 of components such as Gaussian, Student’s t , log-normal, and negative-binomial distributions.

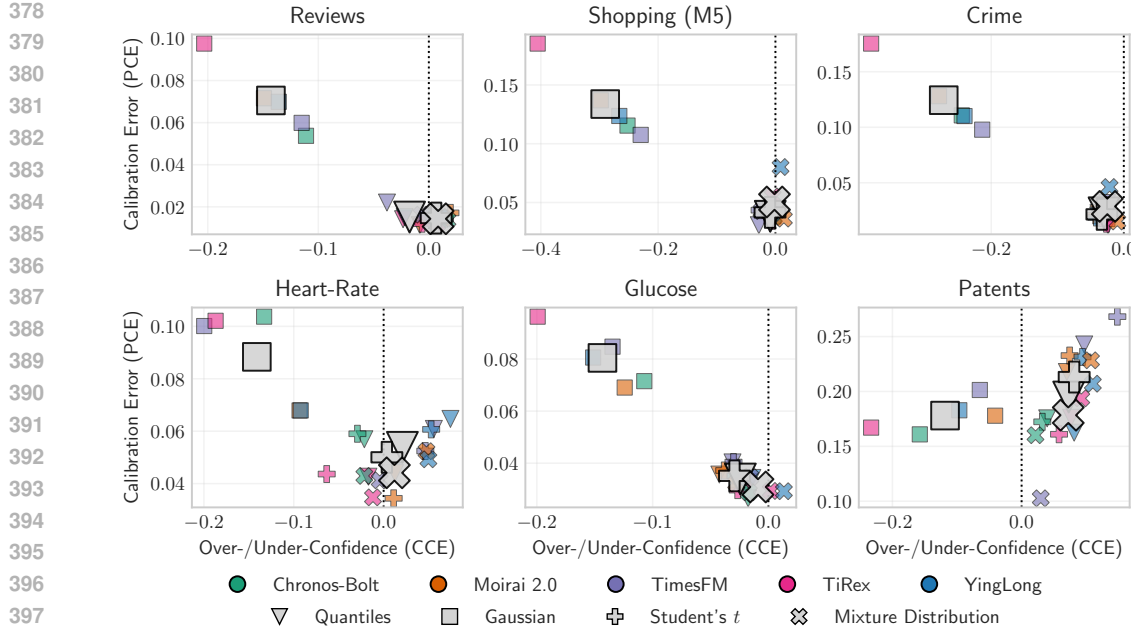


Figure 4: **Gaussian prediction heads are under-confident and are in most cases outperformed by the other prediction heads.** Calibration properties of various prediction heads with Centered Calibration Error (CCE) on the x -axis and Probabilistic Calibration Error (PCE) on the y -axis. Large positive CCE values indicate overconfident predictions, while large negative CCE values show under-confidence. Background markers are the results for each head (shape) with each backbone model (color), while the larger gray centroids are the mean results across models.

An important question is whether the form of a prediction head for a model affects its calibration performance? To address this question, we used the latent information produced by each pretrained TSFM backbone and trained different prediction heads (using TSMixup) for each, specifically: a Gaussian distribution, a Student’s t distribution, and a mixture distribution containing a Gaussian, Student’s t , log-normal, and a Laplace distribution. We also retrained a separate quantile projection head on TSMixup as a control to compare against and found that the trained projection heads correctly learn the latent information of the original foundation model with the trained quantile heads having equivalent forecasting performance as the original quantile head.

We then evaluated all combinations of models and prediction heads using the PCE and CCE metrics. As shown in Figure 4, the **quantile, Student’s t , and mixture distribution heads have very similar calibration error across all datasets**, indicating that there is no significant advantage for any of the three over the others. On the other hand, **the Gaussian distribution’s calibration results are significantly worse** than the other heads. In particular, the Gaussian heads are consistently underconfident with CCE scores (x -axis of Figure 4), always lower than the other heads. This underconfidence also translated to consistently higher calibration error. We speculate that the limited expressiveness of the Gaussian distribution results in poor calibration while the more expressive distributions are better calibrated without suffering from overfitting issues.

4.4 HOW DO AR METHODS AFFECT CALIBRATION IN LONG-TERM FORECASTING?

It is well known that autoregressive (AR) models can deteriorate when making long-term predictions when the desired forecast length H is much longer than the model’s forecast horizon p (Auer et al., 2025). Different approaches to AR forecasting have been proposed, with different tradeoffs in terms of how errors accumulate and how much computational effort is involved. An important question from a calibration perspective is how do the different AR forecasting methods affect calibration performance? To investigate this, we evaluated how calibration properties of TSFMs vary as a function of horizon length p and AR method. We focused primarily on the Chronos-Bolt, TimesFM,

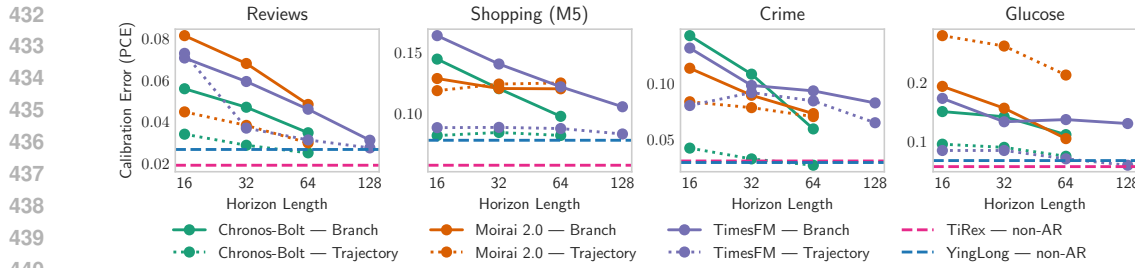


Figure 5: **For long-term AR forecasting, increasing the horizon length and using the trajectory AR method produces better calibrated forecasts.** The figure compares Probabilistic Calibration Error (PCE) for long-term forecasting using autoregression on the y -axis with AR prediction horizon on the x -axis. The color of the line depicts the model used and the line style indicates the AR method. The pink and blue dashed horizontal lines are the PCE for TiRex and YingLong without using AR.

and Moirai 2.0 models in these experiments given that TiRex and YingLong model architectures allow for long-term forecasting natively without requiring AR.

For both the trajectory and branching AR methods, the **predictions with a shorter forecast horizon p have poorer calibration**. This is more pronounced in the branching method, where forecasts with horizon lengths of 16 have notably worse PCE than with 64 or 128 as shown in Figure 5. The trajectory AR approach has generally lower PCE than the branching method when comparing with the same forecast horizon. The explanation for this becomes more clear when viewing CCE from Figure 16 in the Appendix with respect to these methods. **All autoregressive TSFMs are consistently overconfident in long-term forecasting.** While both methods show that shorter forecast horizons results in more confident forecasts, the CCE values for the branching method are often greater than 0.15 for horizon lengths of 16 and 32. This overconfidence reduces steeply as the horizon length increases thus reducing overall calibration error. Although the trajectory method can be more computationally expensive than the branching approach, our results indicate that the trajectory method is better calibrated for long-term forecasting. The non-AR approaches of TiRex and YingLong are significantly more efficient than both AR methods, and they tend to be better calibrated and were not significantly over- or under-confident. Future work in long-term forecasting should prioritize models with longer forecast horizons and alternatives to AR-based approaches.

5 CONCLUSION

Understanding the calibration properties of TSFMs closes a gap in the literature, which has primarily focused to date on point accuracy. Calibration is crucial, however, to accurately quantify the inherent uncertainties associated with time-series forecasting.

In this paper, we evaluated the calibration properties of current leading TSFMs and found that they are consistently well-calibrated relative to the N-BEATS and ARIMA baselines. Unlike the baselines, which are under-confident, the TSFMs show no signs of systematic over- or under-confidence in short-term forecasting. When replacing the projection heads of the TSFMs, the Gaussian prediction head results in consistently under-confident forecasts across the different model backbones, while other distribution and quantile heads are all well-calibrated without significant differences. For long-term forecasting using autoregression, having larger prediction horizons and using the trajectory AR approach over the branching method decrease calibration error and reduces overconfidence.

A limitation of our study is that our evaluations only considered TSFMs for zero-shot univariate time series and calibration relative to a fixed set of quantiles $q \in \{0.1, \dots, 0.9\}$. As such, worthwhile extensions of our work could be to investigate calibration in the context of fine-tuning, to extend multivariate data, and to examine higher-resolution quantiles. Another important practical direction for future investigation is how distribution shift and non-stationarity may affect the calibration performance of both TSFMs and baselines, given the well-known sensitivity of the calibration performance of deep classification models to distribution shift (Ovadia et al., 2019).

486 REFERENCES
487

- 488 Taha Aksu, Gerald Woo, Juncheng Liu, Xu Liu, Chenghao Liu, Silvio Savarese, Caiming Xiong,
489 and Doyen Sahoo. Gift-eval: A benchmark for general time series forecasting model evaluation.
490 *arXiv preprint arXiv:2410.10393*, 2024.
- 491 Abdul Fatir Ansari, Lorenzo Stella, Caner Turkmen, Xiyuan Zhang, Pedro Mercado, Huibin Shen,
492 Oleksandr Shchur, Syama Sundar Rangapuram, Sebastian Pineda Arango, Shubham Kapoor, et al.
493 Chronos: Learning the language of time series. *Transactions on Machine Learning*, November
494 2024a.
- 495 Abdul Fatir Ansari, Caner Turkmen, Oleksandr Shchur, and Lorenzo Stella. Fast and
496 accurate zero-shot forecasting with Chronos-Bolt and AutoGluon, Dec 2024b. URL
497 <https://aws.amazon.com/blogs/machine-learning/fast-and-accurate-zero-shot-forecasting-with-chronos-bolt-and-autogluon/>.
- 498
- 499 Andreas Auer, Patrick Podest, Daniel Klotz, Sebastian Böck, Günter Klambauer, and Sepp Hochreiter.
500 Tirex: Zero-shot forecasting across long and short horizons with enhanced in-context learning.
501 *arXiv preprint arXiv:2505.23719*, 2025.
- 502
- 503 Maximilian Beck, Korbinian Pöppel, Markus Spanring, Andreas Auer, Oleksandra Prudnikova,
504 Michael Kopp, Günter Klambauer, Johannes Brandstetter, and Sepp Hochreiter. xLSTM: Ex-
505 tended long short-term memory, 2024. URL <https://arxiv.org/abs/2405.04517>.
- 506
- 507 Konstantinos Benidis, Syama Sundar Rangapuram, Valentin Flunkert, Yuyang Wang, Danielle Mad-
508 dix, Caner Turkmen, Jan Gasthaus, Michael Bohlke-Schneider, David Salinas, Lorenzo Stella,
509 et al. Deep learning for time series forecasting: Tutorial and literature survey. *ACM Computing
Surveys*, 55(6):1–36, 2022.
- 510
- 511 Rishi Bommasani, Drew A Hudson, Ehsan Adeli, Russ Altman, Simran Arora, Sydney von Arx,
512 Michael S Bernstein, Jeannette Bohg, Antoine Bosselut, Emma Brunskill, et al. On the opportu-
513 nities and risks of foundation models. *arXiv preprint arXiv:2108.07258*, 2021.
- 514
- 515 Glenn W Brier. Verification of forecasts expressed in terms of probability. *Monthly Weather Review*,
516 78(1):1–3, 1950.
- 517
- 518 Peter Cho, Juseong Kim, Brinnae Bent, and Jessilyn Dunn. Big ideas lab glycemic variability and
wearable device data. (*version 1.1. 1*). *PhysioNet*, 2023.
- 519
- 520 Youngseog Chung, Willie Neiswanger, Ian Char, and Jeff Schneider. Beyond pinball loss: Quantile
521 methods for calibrated uncertainty quantification. *Advances in Neural Information Processing
Systems*, 34:10971–10984, 2021.
- 522
- 523 Ben Cohen, Emaad Khwaja, Youssef Doubli, Salahidine Lemaachi, Chris Lettieri, Charles Masson,
524 Hugo Miccinilli, Elise Ramé, Qiqi Ren, Afshin Rostamizadeh, et al. This time is different: An
525 observability perspective on time series foundation models. *arXiv preprint arXiv:2505.14766*,
526 2025.
- 527
- 528 Benjamin F Crabtree, Subhash C Ray, Priscilla M Schmidt, Patrick T O’Connor, and David D
529 Schmidt. The individual over time: time series applications in health care research. *Journal of
Clinical Epidemiology*, 43(3):241–260, 1990.
- 530
- 531 Abhimanyu Das, Weihao Kong, Rajat Sen, and Yichen Zhou. A decoder-only foundation model
532 for time-series forecasting. In *Proceedings of the 41st International Conference on Machine
Learning*, 2024.
- 533
- 534 Chirag Deb, Fan Zhang, Junjing Yang, Siew Eang Lee, and Kwok Wei Shah. A review on time series
535 forecasting techniques for building energy consumption. *Renewable and Sustainable Energy
Reviews*, 74:902–924, 2017.
- 536
- 537 Victor Dheur and Souhaib Ben Taieb. A large-scale study of probabilistic calibration in neural
538 network regression. In *International Conference on Machine Learning*, pp. 7813–7836. PMLR,
539 2023.

- 540 Marian Farah, Paul Birrell, Stefano Conti, and Daniela De Angelis. Bayesian emulation and cali-
 541 bration of a dynamic epidemic model for a/h1n1 influenza. *Journal of the American Statistical*
 542 *Association*, 109(508):1398–1411, 2014.
- 543
- 544 Tilman Gneiting and Adrian E Raftery. Strictly proper scoring rules, prediction, and estimation.
 545 *Journal of the American statistical Association*, 102(477):359–378, 2007.
- 546 Tilman Gneiting, Fadoua Balabdaoui, and Adrian E Raftery. Probabilistic forecasts, calibration
 547 and sharpness. *Journal of the Royal Statistical Society Series B: Statistical Methodology*, 69(2):
 548 243–268, 2007.
- 549 Sharad Goel, Jake M Hofman, Sébastien Lahaie, David M Pennock, and Duncan J Watts. Predicting
 550 consumer behavior with Web search. *Proceedings of the National Academy of Sciences*, 107(41):
 551 17486–17490, 2010.
- 552
- 553 Xiao Gu, Yu Liu, Zaineb Mohsin, Jonathan Bedford, Anshul Thakur, Peter Watkinson, Lei Clifton,
 554 Tingting Zhu, and David Clifton. Are time series foundation models ready for vital sign forecast-
 555 ing in healthcare? In *Proceedings of the 4th Machine Learning for Health Symposium*, volume
 556 259 of *Proceedings of Machine Learning Research*, pp. 401–419. PMLR, 15–16 Dec 2025.
- 557
- 558 Chuan Guo, Geoff Pleiss, Yu Sun, and Kilian Q Weinberger. On calibration of modern neural
 559 networks. In *International Conference on Machine Learning*, pp. 1321–1330. PMLR, 2017.
- 560
- 561 James D Hamilton. *Time Series Analysis*. Princeton University Press, 1994.
- 562
- 563 Hans Hersbach. Decomposition of the continuous ranked probability score for ensemble prediction
 564 systems. *Weather and Forecasting*, 15(5):559–570, 2000.
- 565
- 566 Yupeng Hou, Jiacheng Li, Zhankui He, An Yan, Xiusi Chen, and Julian McAuley. Bridging language
 567 and items for retrieval and recommendation. *arXiv preprint arXiv:2403.03952*, 2024.
- 568
- 569 Rob J Hyndman and Yeasmin Khandakar. Automatic time series forecasting: the forecast package
 570 for R. *Journal of Statistical Software*, 27:1–22, 2008.
- 571
- 572 Robin John Hyndman and George Athanasopoulos. *Forecasting: Principles and Practice*. OTexts,
 573 Australia, 2nd edition, 2018.
- 574
- 575 Zhengbao Jiang, Jun Araki, Haibo Ding, and Graham Neubig. How can we know when language
 576 models know? on the calibration of language models for question answering. *Transactions of the*
 577 *Association for Computational Linguistics*, 9:962–977, 2021.
- 578
- 579 Sanyam Kapoor, Nate Gruver, Manley Roberts, Arka Pal, Samuel Dooley, Micah Goldblum, and
 580 Andrew Wilson. Calibration-tuning: Teaching large language models to know what they don’t
 581 know. In *Proceedings of the 1st Workshop on Uncertainty-Aware NLP (UncertaiNLP 2024)*, pp.
 582 1–14, 2024.
- 583
- 584 Volodymyr Kuleshov, Nathan Fenner, and Stefano Ermon. Accurate uncertainties for deep learning
 585 using calibrated regression. In *International Conference on Machine Learning*, pp. 2796–2804.
 586 PMLR, 2018.
- 587
- 588 Jiacheng Li, Jingbo Shang, and Julian McAuley. UCTopic: Unsupervised contrastive learning for
 589 phrase representations and topic mining. *arXiv preprint arXiv:2202.13469*, 2022.
- 590
- 591 Yuxuan Liang, Haomin Wen, Yuqi Nie, Yushan Jiang, Ming Jin, Dongjin Song, Shirui Pan, and
 592 Qingsong Wen. Foundation models for time series analysis: A tutorial and survey. In *Proceedings*
 593 *of the 30th ACM SIGKDD Conference on Knowledge Discovery and Data Mining*, pp. 6555–
 6565, 2024.
- 594
- 595 Spyros Makridakis, Evangelos Spiliotis, and Vassilios Assimakopoulos. The m4 competition:
 596 100,000 time series and 61 forecasting methods. *International Journal of Forecasting*, 36(1):
 597 54–74, 2020.
- 598
- 599 Spyros Makridakis, Evangelos Spiliotis, and Vassilios Assimakopoulos. The M5 competition: Back-
 600 ground, organization, and implementation. *International Journal of Forecasting*, 38(4):1325–
 601 1336, 2022.

- 594 Alan C Marco, Michael Carley, Steven Jackson, and Amanda Myers. The USPTO historical patent
 595 data files two centuries of innovation, 2015.
- 596
- 597 Benjamin M. Marlin, David C. Kale, Robinder G. Khemani, and Randall C. Wetzel. Unsupervised
 598 pattern discovery in electronic health care data using probabilistic clustering models. In *Proceed-
 599 ings of the 2nd ACM SIGKDD International Health Informatics Symposium*, IHI '12, pp. 389–398,
 600 New York, NY, USA, 2012. Association for Computing Machinery.
- 601 Aditya Krishna Menon and Robert C Williamson. A loss framework for calibrated anomaly de-
 602 tection. In *Proceedings of the 32nd International Conference on Neural Information Processing
 603 Systems*, pp. 1494–1504, 2018.
- 604 Sabrina J Mielke, Arthur Szlam, Emily Dinan, and Y-Lan Boureau. Reducing conversational agents'
 605 overconfidence through linguistic calibration. *Transactions of the Association for Computational
 606 Linguistics*, 10:857–872, 2022.
- 607
- 608 Manfred Mudelsee. *Climate Time Series Analysis: Classical Statistical and Bootstrap Methods*,
 609 volume 51. Springer, 2014.
- 610 New York City Police Department. NYPD Complaint Data Historic, 2025. URL
 611 [https://data.cityofnewyork.us/Public-Safety/NYPD-Complaint-Data-
 612 Historic/qgea-i56i/about_data](https://data.cityofnewyork.us/Public-Safety/NYPD-Complaint-Data-Historic/qgea-i56i/about_data).
- 613
- 614 Yuqi Nie, Nam H Nguyen, Phanwadee Sinthong, and Jayant Kalagnanam. A time series is worth 64
 615 words: Long-term forecasting with transformers. In *The Eleventh International Conference on
 616 Learning Representations*, 2023.
- 617 Boris N Oreshkin, Dmitri Carpow, Nicolas Chapados, and Yoshua Bengio. N-BEATS: Neural ba-
 618 sis expansion analysis for interpretable time series forecasting. In *International Conference on
 619 Learning Representations*, 2019.
- 620 Yaniv Ovadia, Emily Fertig, Jie Ren, Zachary Nado, David Sculley, Sebastian Nowozin, Joshua
 621 Dillon, Balaji Lakshminarayanan, and Jasper Snoek. Can you trust your model's uncertainty?
 622 evaluating predictive uncertainty under dataset shift. *Advances in Neural Information Processing
 623 Systems*, 32, 2019.
- 624
- 625 C.-K Peng, Joseph E Mietus, Yanhui Liu, Gurucharan Khalsa, Pamela S Douglas, Herbert Benson,
 626 and Ary L Goldberger. Exaggerated heart rate oscillations during two meditation techniques.
 627 *International Journal of Cardiology*, 70(2):101–107, 1999.
- 628
- 629 Fotios Petropoulos, Daniele Apiletti, Vassilios Assimakopoulos, Mohamed Zied Babai, Devon K
 630 Barrow, Souhaib Ben Taieb, Christoph Bergmeir, Ricardo J Bessa, Jakub Bijak, John E Boylan,
 631 et al. Forecasting: theory and practice. *International Journal of Forecasting*, 38(3):705–871,
 2022.
- 632
- 633 Francesco Pinto, Philip HS Torr, and Puneet K. Dokania. An impartial take to the CNN vs trans-
 634 former robustness contest. In *European Conference on Computer Vision*, pp. 466–480. Springer,
 2022.
- 635
- 636 Colin Raffel, Noam Shazeer, Adam Roberts, Katherine Lee, Sharan Narang, Michael Matena, Yanqi
 637 Zhou, Wei Li, and Peter J Liu. Exploring the limits of transfer learning with a unified text-to-text
 638 transformer. *Journal of Machine Learning Research*, 21(140):1–67, 2020.
- 639
- 640 Kashif Rasul, Arjun Ashok, Andrew Robert Williams, Hena Ghonia, Rishika Bhagwatkar, Arian
 641 Khorasani, Mohammad Javad Darvishi Bayazi, George Adamopoulos, Roland Riachi, Nadhir
 642 Hassen, et al. Lag-Llama: Towards foundation models for probabilistic time series forecasting.
arXiv preprint arXiv:2310.08278, 2023.
- 643
- 644 Hao Song, Tom Diethe, Meelis Kull, and Peter Flach. Distribution calibration for regression. In
 645 *International Conference on Machine Learning*, pp. 5897–5906. PMLR, 2019.
- 646
- 647 Ibrahim Taha Aksu, Juncheng Liu, Chenghao Liu, Doyen Sahoo, Junnan Li, Caiming Xiong, and
 Silvio Savarese. Introducing Moirai 2.0, Aug 2025. URL <https://www.salesforce.com/blog/moirai-2-0>.

- 648 Ruey S Tsay. *Analysis of Financial Time Series*. John Wiley & Sons, 2005.
649
- 650 Xue Wang, Tian Zhou, Jinyang Gao, Bolin Ding, and Jingren Zhou. Output scaling: YingLong-
651 delayed chain of thought in a large pretrained time series forecasting model, 2025. URL <https://arxiv.org/abs/2506.11029>.
652
- 653 Gerald Woo, Chenghao Liu, Akshat Kumar, Caiming Xiong, Silvio Savarese, and Doyen Sahoo.
654 Unified training of universal time series forecasting transformers. In *Proceedings of the 41st*
655 *International Conference on Machine Learning*, ICML'24. JMLR.org, 2024.
656
- 657 Miao Xiong, Zhiyuan Hu, Xinyang Lu, YIFEI LI, Jie Fu, Junxian He, and Bryan Hooi. Can LLMs
658 express their uncertainty? an empirical evaluation of confidence elicitation in LLMs. In *The*
659 *Twelfth International Conference on Learning Representations*, 2024.
660
- 661 Jiexia Ye, Weiqi Zhang, Ke Yi, Yongzi Yu, Ziyue Li, Jia Li, and Fugee Tsung. A survey of time
662 series foundation models: Generalizing time series representation with large language model.
arXiv preprint arXiv:2405.02358, 2024.
663
- 664 Wenqian Ye, Yunsheng Ma, Xu Cao, and Kun Tang. Mitigating transformer overconfidence via
665 Lipschitz regularization. In *Uncertainty in Artificial Intelligence*, pp. 2422–2432. PMLR, 2023.
666
- 667 Haoyi Zhou, Shanghang Zhang, Jieqi Peng, Shuai Zhang, Jianxin Li, Hui Xiong, and Wancai Zhang.
668 Informer: Beyond efficient transformer for long sequence time-series forecasting. In *Proceedings*
669 *of the AAAI Conference on Artificial Intelligence*, volume 35, pp. 11106–11115, 2021.
670
671
672
673
674
675
676
677
678
679
680
681
682
683
684
685
686
687
688
689
690
691
692
693
694
695
696
697
698
699
700
701

702
703 A APPENDIX704 A.1 LLM USAGE STATEMENT
705706 LLMs were used by the authors as a tool to assist in producing code for experiments. LLMs were
707 not used to aid in the writing of the paper or during research ideation.708
709 A.2 ADDITIONAL DETAILS ON EXPERIMENTAL SETUP
710711 We report the default experiment parameters used in the main paper results in the following table,
712 where the train/test split size varies by dataset, with train sets containing approximately 700 time
713 steps per time series:714
715 Table 2: Experimental setup details per dataset.

	Prediction Length (H)	Context Size (T)	Seasonality (ARIMA only)	Train/test split
Reviews	64	512	24	2020-01-31 23:00
Shopping (M5)	64	512	7	2015-04-23
Glucose	64	512	1	2020-02-16 12:43
Heart-Rate	64	128	1	2000-01-01 00:04:59
Crime	64	512	7	2015-01-01
Patents	64	128	1	2004-01-01

725 Prediction length is fixed at 64 time steps across all datasets for short-term forecasting experiments
726 while long-term forecasting experiments used a desired forecast length of 256 time steps.727 Baseline models (N-BEATS and ARIMA) use the training data (dates before train/test split column)
728 for parameter selection and training. The train/test split was determined based on the minimal size
729 of the train set for training N-BEATS and ARIMA models, limited by time series length. Models
730 forecast the first 64 time steps of the test set using the end of the training set as the context. The
731 forecast date and non-AR context are then shifted by the stride, forecasting an additional 64 time-
732 steps. The models forecast repeatedly until the end of the time series. For a stride $d \in \{1, 4, 8\}$
733 dependent on time series length, the first forecast predicts $\hat{y}_{T+1:T+H} | y_{1:T}$ while the second forecast
734 is shifted by the stride to $\hat{y}_{T+1+d:T+H+d} | y_{1+d:T+d}$.735 Seasonality is a hyperparameter for the ARIMA models, used for initialization. We limit the max lag
736 (context) for the ARIMA model to 64 for all datasets. We train an ARIMA model with AutoARIMA
737 on the train set and then use the selected hyperparameters to train the models for evaluation. We train
738 a new ARIMA model each time we shift the context.739 For N-BEATS we perform a grid search on a variety of hyperparameters (see Table 3) using the
740 training data and select the model with the lowest WQL on the same data. Quantile loss outperforms
741 normal distribution loss on all datasets. When forecasting with distribution loss in N-BEATS, we
742 use the default 100 samples. We train a single N-BEATS model on each dataset, training across
743 multiple time series and reuse the same learned parameters each time we shift the context.744
745 Table 3: N-BEATS hyperparameter grid search space.

Hyperparameter	Search Space
Epochs	{100, 1000}
Learning Rate	{0.001, 0.0001}
Early Stop Patience Steps	{-1, 2}
Number of Blocks	{(1,1,1), (3,3,3)}
Validation Check Steps	{10, 100}
Loss Function	{Normal Distribution Loss, Quantile Loss}

754
755 We describe the AR methods in depth in the next section and used $n = 100$ as the number of
trajectories for the trajectory AR method. When sampling from the quantile heads in the trajec-

756 tory method, we linearly interpolate between the quantiles to convert the quantile heads into to a
 757 continuous distribution.
 758

759 **A.3 AUTOREGRESSIVE METHODS**
 760

761 The **naive** AR method used by TimesFM and Chronos-Bolt adds only the median or mean forecasts
 762 to the context. For example if the desired forecast length is $H = 256$ and the model’s forecast
 763 horizon is $p = 64$, the model will generate a probabilistic forecast $\hat{y}_{T+1:T+64}$ given the observed
 764 context $y_{1:T}$. To make the next 64-step forecast, it adds the mean or median forecast, derived from
 765 $\hat{y}_{T+1:T+64}$, to the original context. The result is a shifted context $y_{65:T+64}$ containing a mix of
 766 observed values and forecasted values. The model can then use the shifted context to produce the
 767 forecasts for $\hat{y}_{T+65:T+128}$. This process is repeated until all 256 probabilistic forecasts have been
 768 completed, and the quantiles can be obtained directly from the probabilistic forecasts.

769 The **branching** approach from Moirai 2.0 is different in that it requires the model to forecast the
 770 same time steps multiple times. The first 64 time steps is normal, relying only on the observed
 771 contexts and producing $|Q|$ quantile forecasts $\hat{y}_{T+1:T+64}^q$, where $q \in Q$. The context is duplicated
 772 or branched into $|Q|$ new extended contexts, where each context is extended by the forecasts at a
 773 specific quantile. The next 64 steps $\hat{y}_{T+65:T+128}^q$ is forecasted using all $|Q|$ contexts, which requires
 774 running the model $|Q|$ times independently, once for each of the $|q|$ contexts. Because the model
 775 has been run $|Q|$ times and each time the model produces $|Q|$ quantiles, there will be a total of
 776 $|Q|^2$ forecasts for each time step. Rather than increasing the number of contexts exponentially from
 777 $|Q|$ to $|Q|^2$, the $|Q|^2$ quantile forecasts at each time step are aggregated back down to a set of $|Q|$
 778 quantile predictions. This is done by taking the Q quantile of the $|Q|^2$ forecasts (for each time step).
 779 These aggregated quantiles become the returned quantile forecasts and are used to extend and shift
 780 the corresponding $|Q|$ contexts.

781 The Toto TSFM (Cohen et al., 2025) uses a **trajectory**-based AR method where the model generates
 782 n independent AR forecasts or trajectories. Each trajectory is produced similarly to the naive method
 783 where a single point forecast (at each time step in p) is added to the context for AR. However, instead
 784 of using the mean or median, the model samples from the predicted density and uses the samples as
 785 the point forecast (one sample for each time step). The model will create n independent trajectories
 786 each with separate contexts. The final quantile forecasts are produced by taking the quantiles of the
 787 n trajectories at each time step independently.

788 **A.4 MODELS**
 789

790 We primarily selected models with diverse backbones that were state-of-the-art on the GIFT-EVAL
 791 benchmark as of the time of writing (Aksu et al., 2024) and pre-trained on time series datasets.
 792

793 **TimesFM** TimesFM (Das et al., 2024) uses a decoder-only stacked transformer architecture,
 794 and provides probabilistic predictions at pre-trained fixed quantile heads. The training objec-
 795 tive combines mean squared error (MSE) and quantile loss Hyndman & Athanasopoulos (2018);
 796 Gneiting et al. (2007). The model is trained with larger output patches than inputs, and thus
 797 able to make joint predictions of forecast quantiles over lengths $H \leq 128$. We use the
 798 timesfm-2.0-500m-pytorch version for our experiments.²
 799

800 **Moirai 2.0** Moirai 2.0 (Taha Aksu et al., 2025) is a recent update on Moirai 1.0 (Woo et al., 2024)
 801 transitioning from an encoder-based transformer that uses a mixture distribution projection head
 802 to a decoder-only backbone with a quantile head. Moirai 2.0 is implemented using AR with multi-
 803 patch forecasting support. In our experiments, we used a patch size of 16 and set the model to jointly
 804 predict 4 patches at a time for a max prediction horizon of 64. We use the moirai-2.0-R-small
 805 version for our experiments.³
 806

807 ²TimesFM checkpoint on Hugging Face: <https://huggingface.co/google/timesfm-2.0-500m-pytorch>.
 808

809 ³Moirai 2.0 checkpoint on Hugging Face: <https://huggingface.co/Salesforce/moirai-2.0-R-small>

Chronos-Bolt Chronos-Bolt (Ansari et al., 2024b) is a foundation model with an backbone from the T5 family of encoder-decoder language models Raffel et al. (2020). Real-valued time series is tokenized into fixed vocabularies via scaling and quantization. Unlike its predecessor Chronos (Ansari et al., 2024a) which used a categorical prediction head forecasting the tokenized patches within a set vocabulary, Chronos-Bolt directly predicts quantiles using an output patch length of 64. We use the `chronos-bolt-base` version for our experiments.⁴

TiRex TiRex (Auer et al., 2025) deviates from most TSFMs by using an xLSTM (Beck et al., 2024) decoder-only backbone. They apply contiguous patch masking during pretraining to allow for long-term forecasting without the need for AR. For long-term forecasts at inference time, TiRex pads and shifts the context so that the model does not need to condition on previous forecasts. Their implementation allows for multi-patch accelerated roll-out by using the forecasts at multiple patches in single forward pass, rather than only using a single patch before padding the context. We use the base `TiRex` version for our experiments and set the accelerated roll-out to 4 patches with patch size of 32.⁵

YingLong YingLong (Wang et al., 2025) employs a bi-directional U-net encoder-only transformer backbone. This enables the model to use delayed chain-of-thought reasoning by forecasting beyond the desired forecast length. The desired forecast can then condition on both the observed context and the future delayed chain-of-thought for more accurate predictions. We use the `YingLong_110m` version for our experiments and use an extended forecast horizon of 2048.⁶

N-BEATS N-BEATS (Oreshkin et al., 2019) is a deep neural architecture that has been designed for the purposes of time series predictions. Similarly to TimesFM, N-BEATS jointly forecasts the entire prediction horizon in a single forward pass.

ARIMA We use Nixtla’s `StatsForecast` implementation of AutoARIMA (Hyndman & Khandakar, 2008) to automatically select the optimal ARIMA parameters for each time series on the training set. The model is then refit on all earlier data before each forecast on the evaluation set. The ARIMA implementation uses Kalman filters to recursively predict the mean and variance. Quantiles are computed by fitting a normal distribution to the forecasts and using the inverse CDF (PPF) with the appropriate z -scores.

A.5 PREDICTION HEADS

To evaluate the impact the prediction head has on calibration, we replaced the default quantile projection heads of each model with a fine-tuned version of each head we tested. To train each head, we cached the embeddings outputted by each model’s backbones and used them as the input to each of the heads. Specifically, we trained an independent quantile, Gaussian, Student’s t , and mixture distribution head. For the mixture head we replicate the Moirai 1.0 (Woo et al., 2024) prediction head using a Gaussian, Student’s t , log-normal, and replace Negative-Binomial with the Laplace distribution due to issues related to model convergence during training.

A.6 DATASETS

We evaluate models on three human behavior datasets: (i) a **Reviews** dataset consisting of hourly counts of Amazon product reviews (Hou et al., 2024) and Google Places reviews (Li et al., 2022), (ii) a modified **Shopping (M5)** dataset (Makridakis et al., 2022) consisting of the daily number of products being sold at different locations, and (iii) an NYC **Crime** report dataset (New York City Police Department, 2025) aggregating daily crime occurrences.

For the **Reviews** ensemble dataset, we aggregated Amazon Hou et al. (2024) and Google Li et al. (2022) reviews by product and location category and sampled 239 of the most abundant categories

⁴Chronos-Bolt checkpoint on Hugging Face: <https://huggingface.co/amazon/chronos-bolt-base>

⁵TiRex checkpoint on Hugging Face: <https://huggingface.co/NX-AI/TiRex>

⁶YingLong checkpoint on Hugging Face: https://huggingface.co/qcw2333/YingLong_110m

864 from the ensemble. We binned the event data as count data at an hourly granularity and trimmed the
 865 dataset to the most active time range from 2020-01-01 08:00:00 to 2021-06-25 23:00.
 866

867 We aggregated the daily **Shopping (M5)** Makridakis et al. (2022) dataset to reduce sparsity by
 868 binning each product by their product department and store ID, totaling 70 time series.
 869

870 We aggregated the **NYC Crime** reports dataset New York City Police Department (2025) by number
 871 of daily reports and cutoff the dataset to only include reports between the years 2006 and 2023. We
 872 split the dataset into time series based on borough.
 873

874 Many datasets used in training TSFMs are related to human behavior and natural phenomena that
 875 exhibit periodic trends (e.g., 24-hour effects). As noted in Gu et al. (2025), the strong predictive
 876 accuracy of foundation models on many of the datasets used in machine learning evaluations does
 877 not necessarily translate into high predictive accuracy in applications such as vital sign forecasting
 878 in healthcare. To analyze model performance on datasets that differ in this respect from the pre-
 879 training data, we further included datasets for **Glucose Level** (Cho et al., 2023) and **Heart Rate**
 880 prediction (Peng et al., 1999).
 881

882 The **Glucose** Cho et al. (2023) dataset measures interstitial glucose concentration of 16 subjects over
 883 the course of 10 days. We used the Dexcom G6 dataset measuring interstitial glucose concentration
 884 (mg/dL) every 5 minutes.
 885

886 The meditative **Heart-Rate** dataset Peng et al. (1999) records heart-rate of 14 volunteers during a
 887 10-minute metronomic breathing meditation session, where it is recorded as relative time since
 888 the start of the meditation session. However, some foundation models (TimesFM) require and use
 889 timestamps for forecasting so we mapped the Heart-Rate dataset to start at 2000-01-01 00:00:00 and
 890 last 10 minutes.
 891

892 To evaluate models on coarser time granularities, we also use the **Patents** dataset (Marco et al., 2015)
 893 which counts the number of US patents filed per month from 1981 to 2014. We removed sparse time
 894 series, aggregated by patent field and category, and filtered out timeseries with a minimum value of
 895 less than 100.
 896

897 Additional dataset statistics can be found in the partial autocorrelation plots in Figure 6. We did not
 898 evaluate the AR experiments on the Heart-Rate and Patents dataset as they did not contain enough
 899 data to accurately assess long-term forecasting calibration.
 900

901 Both synthetic noise datasets were generated as a single time series with length 4367 and the
 902 train/test split at 1440. The IID noise time series was generated using $y_t = \epsilon$ and the noisy first-order
 903 linear process $y_t = \alpha y_{t-1} + (1 - \alpha)\epsilon$ where $\alpha = 0.9$ and ϵ is drawn from the standard normal
 904 distribution $\mathcal{N}(0, 1)$.
 905

906

907

908

909

910

911

912

913

914

915

916

917

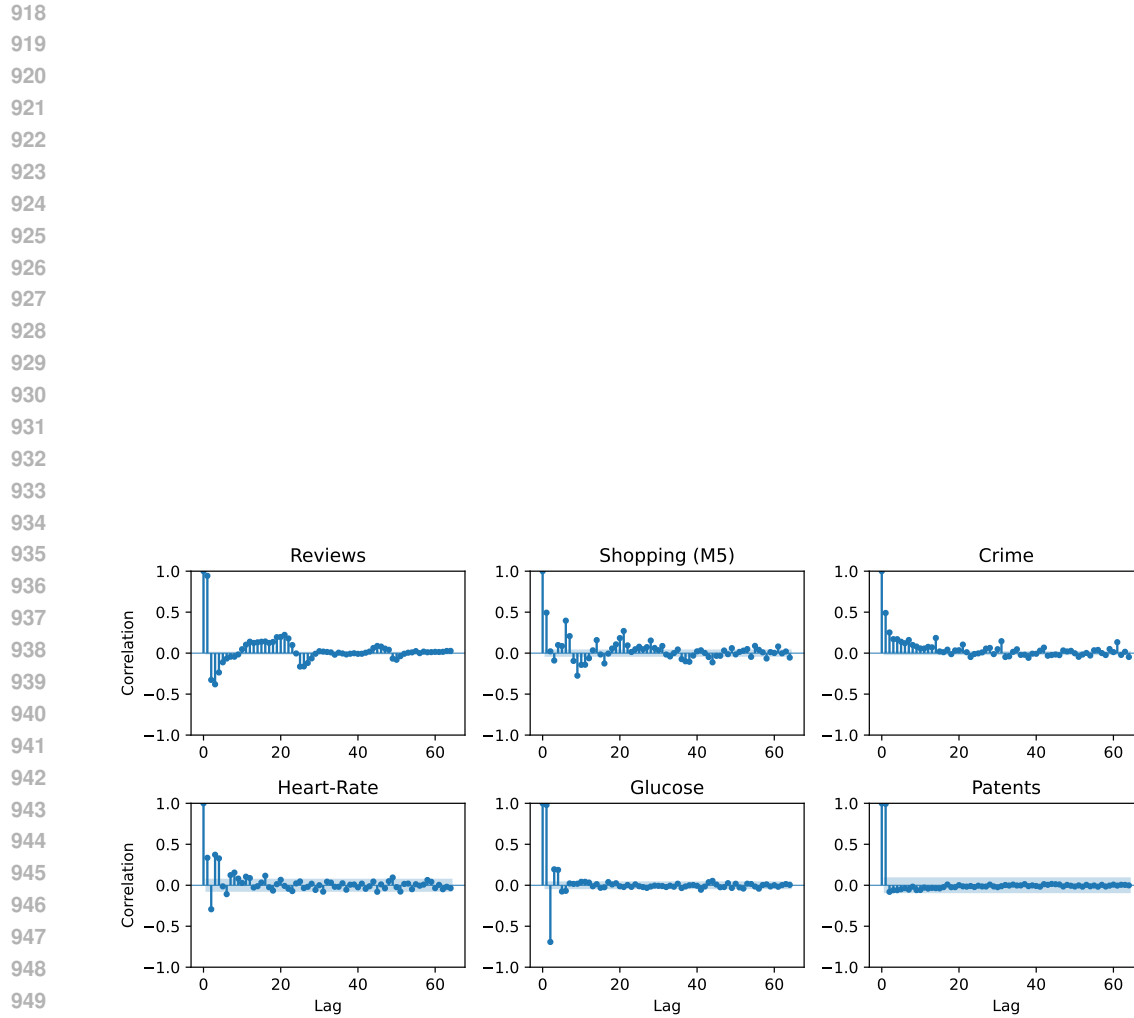
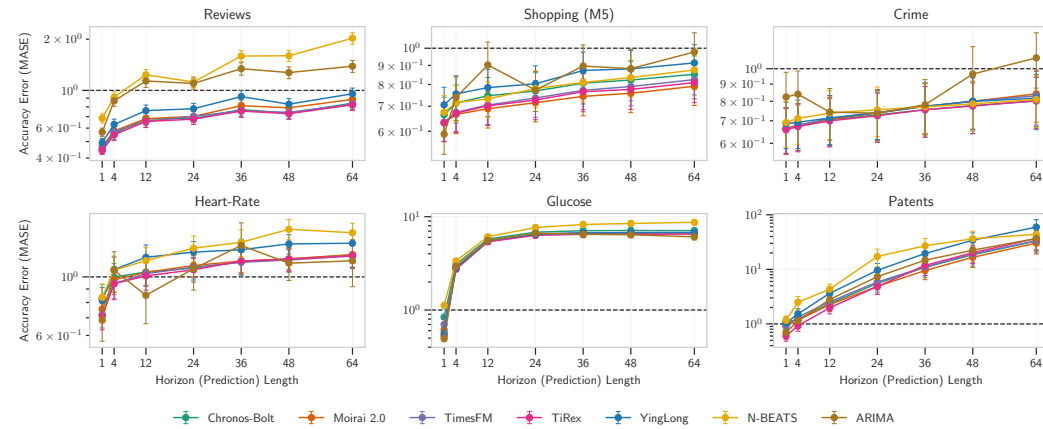


Figure 6: **Partial Autocorrelation Plots: Glucose and Patents datasets have limited number of lags with significant partial autocorrelation while having large correlation at the first lag.** The naive model is well suited for these two datasets which would explain the poor point forecasting performance (MASE). The specific time-series from each dataset used to generate the plots were selected based on having approximately median MASE scores in that dataset.

972 **B ADDITIONAL RESULTS AND FIGURES**
973974 **B.1 BASE FINDINGS**
975976 We include additional figures and findings for each of the experiments below. Table 4 shows the
977 short-term calibration and accuracy scores of each model across all of the datasets.
978979 In Figure 11, we show that across time series in the same dataset, the model point accuracy, MASE,
980 are not correlated with model calibration. However, across datasets as in Figure 9, we see a strong
981 correlation between TSFM, MASE, and PCE with a correlation coefficient of 0.90. This relationship
982 does not always hold. For example, despite the TSFMs having poor point accuracy on the Glucose
983 dataset, worse than a naive predictor with MASE greater than 1.0, they are still well calibrated with
984 PCE less than 0.05. We note that for multi-step predictions ($H > 1$) that the MAE of the naive
985 predictor in the denominator of MASE is in effect using information “from the future,” with the
986 result that the overall MASE may take values greater than 1 even for useful models. In Figures 7
987 and 8, as the TSFMs predict further into the future, not surprisingly the forecasts become both less
988 accurate and less calibrated. We see exceptions in Reviews where the TSFMs remain equally well
989 calibrated up to a forecast length of 64. However, unlike the TSFMs, the baseline models have a
990 consistently high PCE over all prediction lengths.
991992 The TSFMs are not consistently over- nor under-confident (see Figures 3 and 12). However among
993 the TSFMs, YingLong is more confident with tighter intervals compared to the other TSFMs, with
994 some indication of overconfidence on Heart-Rate and Patents datasets.
9951008 **Figure 7: TSFM point accuracy gets increasingly worse the further out the model forecasts**
1009 Mean Absolute Scaled Error (MASE) as a function of prediction length across the six datasets. The
1010 dashed horizontal line is the MASE of the naive predictor ($y_t = y_{t-1}$) as a reference.
1011
1012
1013
1014
1015
1016
1017
1018
1019
1020
1021
1022
1023
1024
1025

1026
1027
1028
1029
1030
1031
1032
1033

1034 Table 4: Calibration evaluation results. Best results are highlighted in bold, and second best results
1035 are underlined.
1036

		Foundation Models					Baselines	
		Chronos-Bolt	Moirai 2.0	TimesFM	TiRex	YingLong	N-BEATS	ARIMA
MASE	Reviews	0.717	0.748	0.720	0.710	0.823	1.416	1.211
	Shopping (M5)	0.785	0.727	0.753	<u>0.743</u>	0.835	0.791	0.854
	Glucose	6.362	5.986	6.051	5.841	6.041	7.326	<u>5.958</u>
	Heart-Rate	1.119	1.118	<u>1.104</u>	1.096	1.257	1.335	1.120
	Crime	<u>0.741</u>	0.759	0.759	0.740	0.761	0.767	0.829
	Patents	<u>11.896</u>	10.639	12.193	12.510	21.297	22.814	14.534
	IID Noise	0.706	<u>0.705</u>	0.707	0.708	0.709	0.926	0.704
	Linear Process	2.491	2.417	<u>2.210</u>	2.325	2.322	2.790	2.166
PCE	Reviews	0.015	0.013	<u>0.012</u>	0.012	0.014	0.061	0.176
	Shopping (M5)	<u>0.033</u>	0.045	0.036	0.031	0.052	0.108	0.131
	Glucose	0.036	<u>0.033</u>	0.050	0.031	0.042	0.092	0.141
	Heart-Rate	0.063	<u>0.051</u>	0.052	0.048	0.077	0.121	0.204
	Crime	0.023	0.035	0.023	<u>0.021</u>	0.014	0.103	0.168
	Patents	<u>0.176</u>	0.154	0.206	0.192	0.259	0.242	0.247
	IID Noise	0.009	<u>0.008</u>	0.004	0.012	0.010	0.072	0.122
	Linear Process	0.033	<u>0.015</u>	0.008	0.022	0.021	0.138	0.122
CCE	Reviews	-0.012	<u>0.007</u>	0.004	-0.013	-0.024	-0.040	-0.351
	Shopping (M5)	<u>0.002</u>	0.000	0.005	-0.026	0.051	-0.203	-0.259
	Glucose	-0.011	-0.050	-0.038	<u>-0.027</u>	0.034	-0.172	-0.280
	Heart-Rate	-0.061	<u>-0.008</u>	0.001	-0.037	0.105	-0.243	-0.411
	Crime	-0.030	-0.020	-0.001	-0.041	<u>0.015</u>	-0.207	-0.337
	Patents	0.028	0.046	0.089	0.069	0.201	0.322	<u>0.031</u>
	IID Noise	<u>0.007</u>	-0.008	0.007	-0.012	0.016	0.111	-0.244
	Linear Process	<u>0.006</u>	-0.020	0.002	-0.021	0.044	0.256	-0.244
SIW	Reviews	0.198	0.204	0.180	0.195	0.248	0.573	1.138
	Shopping (M5)	0.240	0.231	0.241	0.260	0.233	0.538	0.644
	Glucose	0.996	0.972	1.001	0.911	0.761	1.727	1.967
	Heart-Rate	0.716	0.605	0.585	0.653	0.496	1.416	2.174
	Crime	0.278	0.276	0.261	0.290	0.246	0.553	0.852
	Patents	0.108	0.096	0.088	0.086	0.091	0.049	0.092
	IID Noise	0.991	1.035	0.999	1.051	0.977	1.118	2.026
	Linear Process	1.107	1.164	0.985	1.110	0.930	0.629	1.942
WQL	Reviews	56.732	59.070	56.929	56.141	65.569	98.865	128.830
	Shopping (M5)	59.558	55.129	57.137	56.454	63.402	56.402	63.618
	Glucose	61.234	57.926	58.157	<u>56.564</u>	58.398	64.942	56.257
	Heart-Rate	19.410	19.332	18.967	<u>19.011</u>	21.812	22.679	27.851
	Crime	<u>39.293</u>	40.129	40.198	39.426	40.409	37.809	47.707
	Patents	22.549	20.958	24.341	24.435	45.050	47.238	25.886

1073
1074
1075
1076
1077
1078
1079

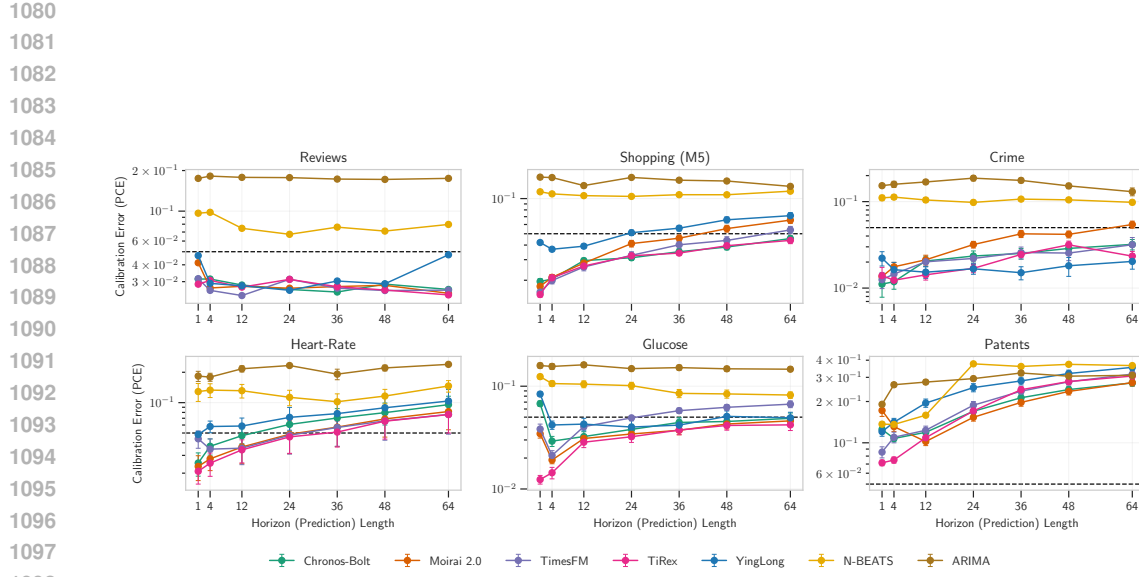


Figure 8: **TSFM calibration gets increasingly worse the further out the model forecasts** Probabilistic Calibration Error (PCE) as a function of prediction length across the six datasets. PCE values below the dashed horizontal line ($y = 0.05$) can be considered to be well-calibrated.

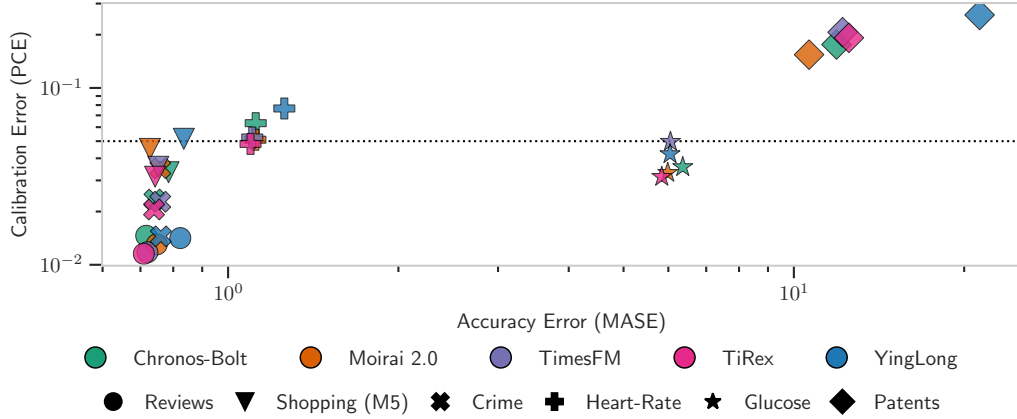


Figure 9: **Aggregated across each dataset TSFMs have a correlation between point accuracy (MASE) and calibration (PCE).** Probabilistic calibration error (PCE) versus point-forecast accuracy (MASE) averaged over all time series in each dataset.

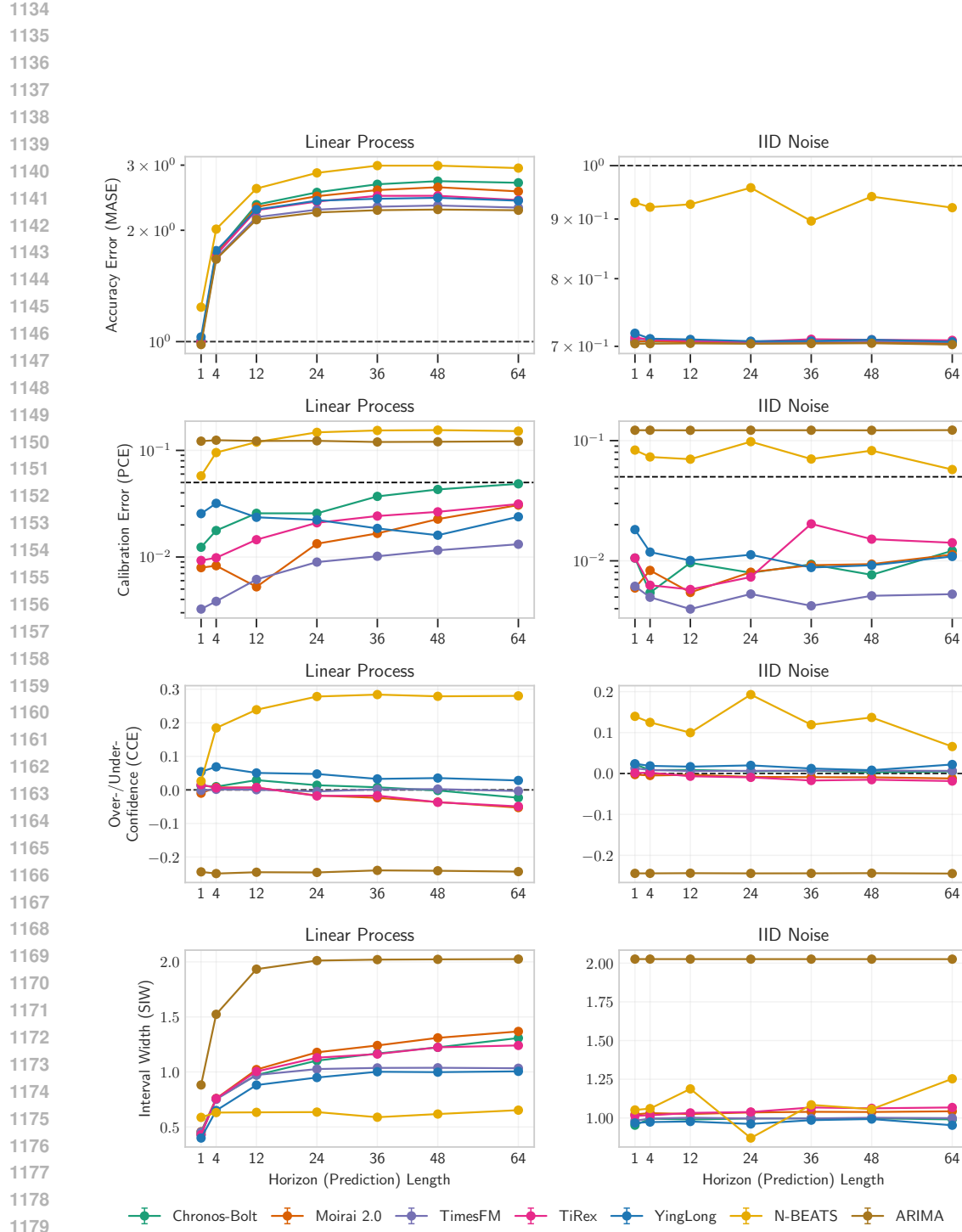


Figure 10: **TSFMs are well calibrated on synthetic datasets while ARIMA is under-confident predicting higher variance (SIW).** Plots calibration and accuracy metrics as a function of horizon length for synthetic datasets.

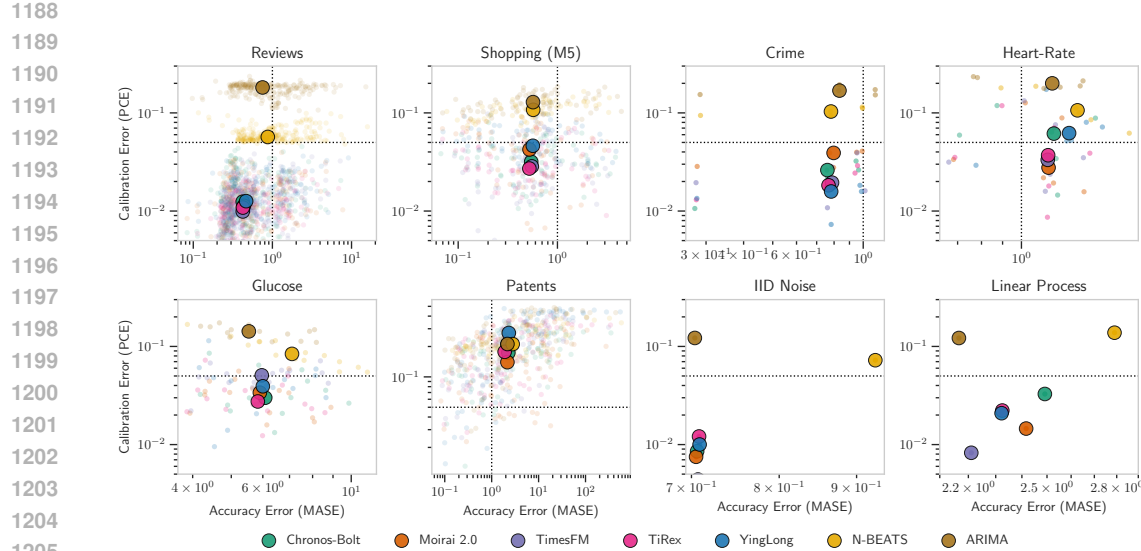


Figure 11: TSFMs are better calibrated than the baselines. Within each dataset, there is no correlation between MASE and PCE. Probabilistic calibration error (PCE) versus point-forecast accuracy (MASE) across the six datasets. Each dot represents model performance on an individual time series; larger centroids being the average over all time series in a dataset. PCE values below 0.05 (dotted horizontal line) are well-calibrated while MASE values less than 1.0 (dotted horizontal line) are better than the naive predictor. MASE values greater than 1.0 can still be a useful model due to the naive model using information “from the future.”

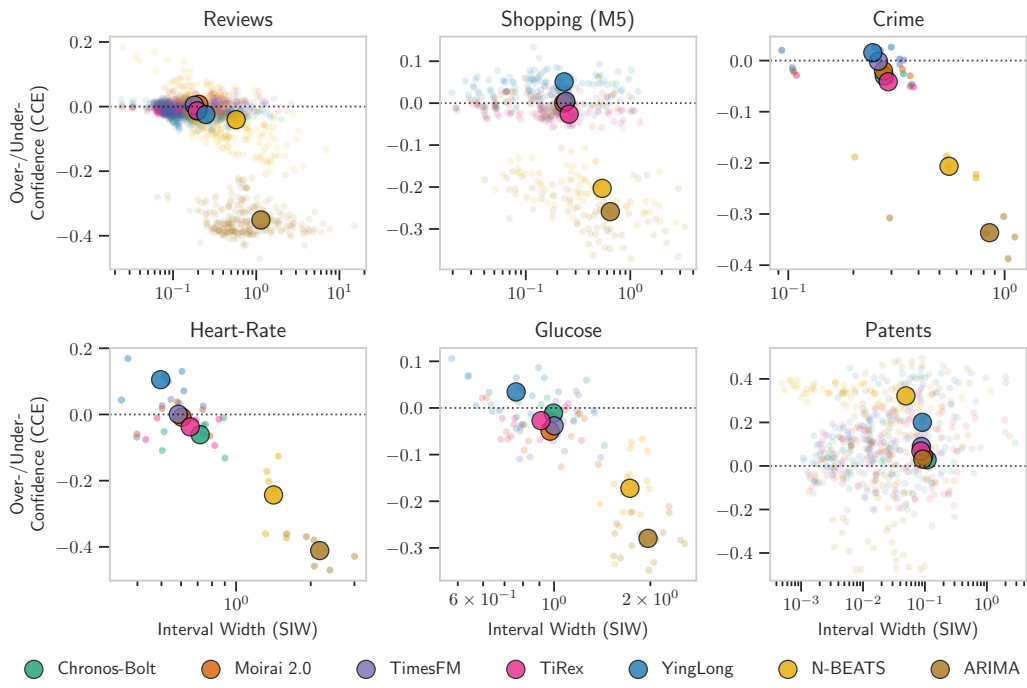


Figure 12: TSFMs tend to be neither over/under-confident overall. Models with larger SIW, wider confidence intervals, were more under-confident. Centered Calibration Error (CCE) versus Scaled Interval Width (SIW) across the six datasets. Each dot represents model performance on an individual time series; larger centroids being the average over all time series in a dataset.

1242 B.2 COMPARISON WITH ADDITIONAL METRICS
1243

1244 As mentioned in the main paper, WQL, MSIS, and CRPS are common metrics for evaluating model
1245 calibration. Weighted Quantile Loss (WQL) is an approximation of Continuous Ranked Probability
1246 Score (CRPS) defined as the pinball (or quantile) loss p_q scaled by the absolute sum of the true
1247 values:

$$1248 \\ 1249 \\ 1250 p_q(y_t, \hat{y}_t^q) = \begin{cases} 2 \cdot (1 - q) \cdot (\hat{y}_t^q - y_t) & \text{if } \hat{y}_t^q \geq y_t \\ 2 \cdot q \cdot (y_t - \hat{y}_t^q) & \text{if } \hat{y}_t^q < y_t \end{cases} \quad (5)$$

$$1252 \\ 1253 WQL = \frac{1}{\sum_{t=T+1}^{T+H} |y_t|} \sum_{t=T+1}^{T+H} \sum_q p_q(y_t, \hat{y}_t^q) \quad (6)$$

1255 However, as described in Chung et al. (2021), CRPS and WQL, measure a combination of prob-
1256 abilistic calibration and sharpness Gneiting et al. (2007). This combination leads to an imbalance
1257 often skewing to prioritize predictive sharpness Chung et al. (2021).

1259 Mean Scaled Interval Score (MSIS) is a scaled version of Mean Interval Score (MIS) which is the
1260 mean difference in upper and lower bound prediction penalized with the error when the true value
1261 lies outside the bounds:

$$1262 \\ 1263 \\ 1264 MSIS = \frac{1}{MAE_n} \frac{1}{H} \sum_{t=T+1}^H (U_t^s - L_t^s) \\ 1265 \\ 1266 \\ 1267 + \frac{2}{1-s} (L_t^s - y_t) \mathbf{1}[y_t < L_t^s] \\ 1268 \\ 1269 + \frac{2}{1-s} (y_t - U_t^s) \mathbf{1}[y_t > U_t^s] \quad (7)$$

1271 MSIS has the same limitations being a measure of interval size with a penalty term for observed
1272 values outside the interval Gneiting et al. (2007); Hyndman & Athanasopoulos (2018); Gneiting &
1273 Raftery (2007). We find that these metrics were highly correlated to MASE in Figure 14. Therefore,
1274 when using these metrics to evaluate calibration, their values result in a measure of sharpness and
1275 accuracy that diverge from a measurement of calibration (see Figure 13). For example, if we evaluate
1276 calibration using WQL or MSIS, we would incorrectly conclude that ARIMA is equally or better
1277 calibrated than the best foundation models on the Glucose dataset as in Figure 1 and 13.

1278
1279
1280
1281
1282
1283
1284
1285
1286
1287
1288
1289
1290
1291
1292
1293
1294
1295

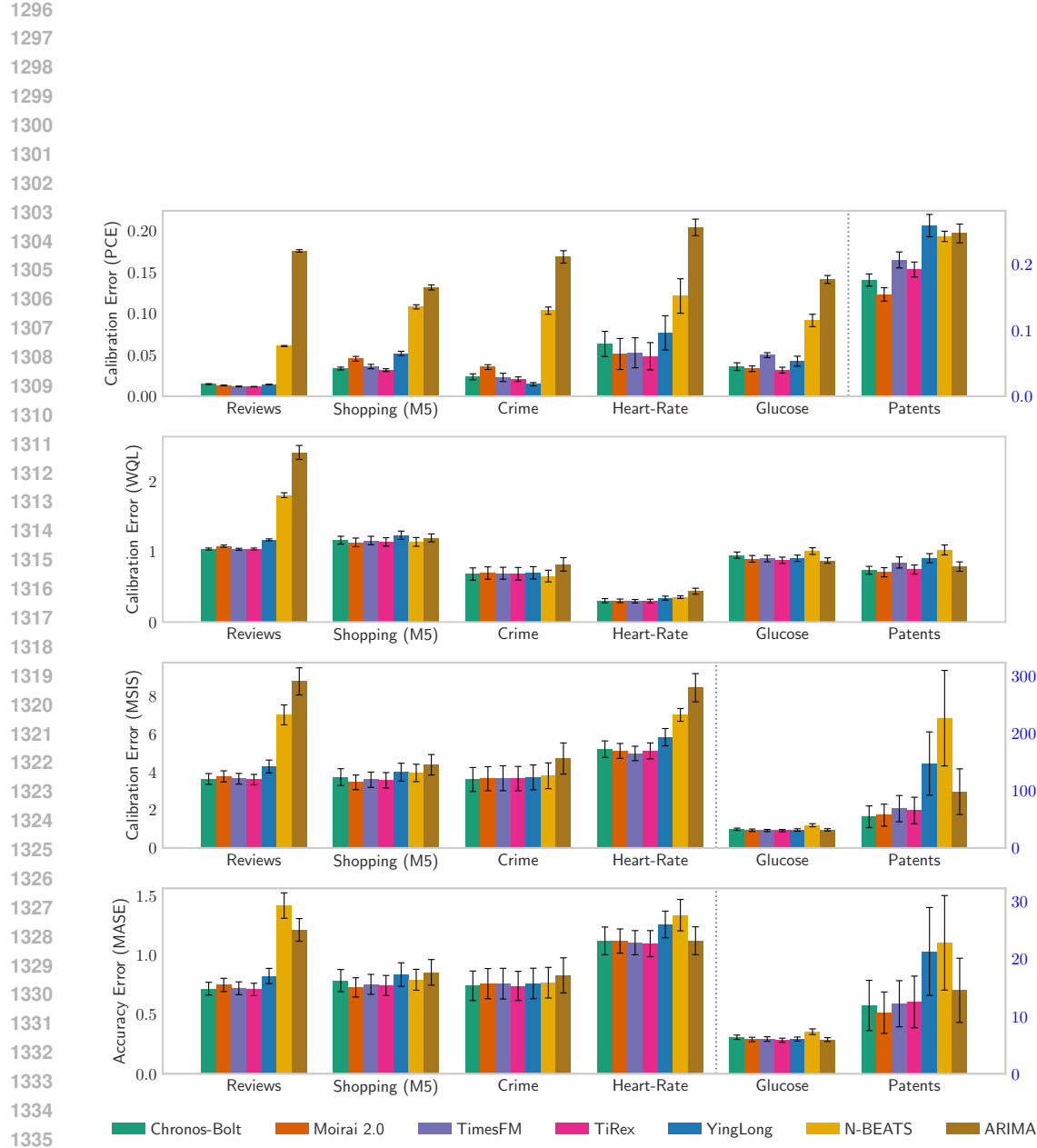
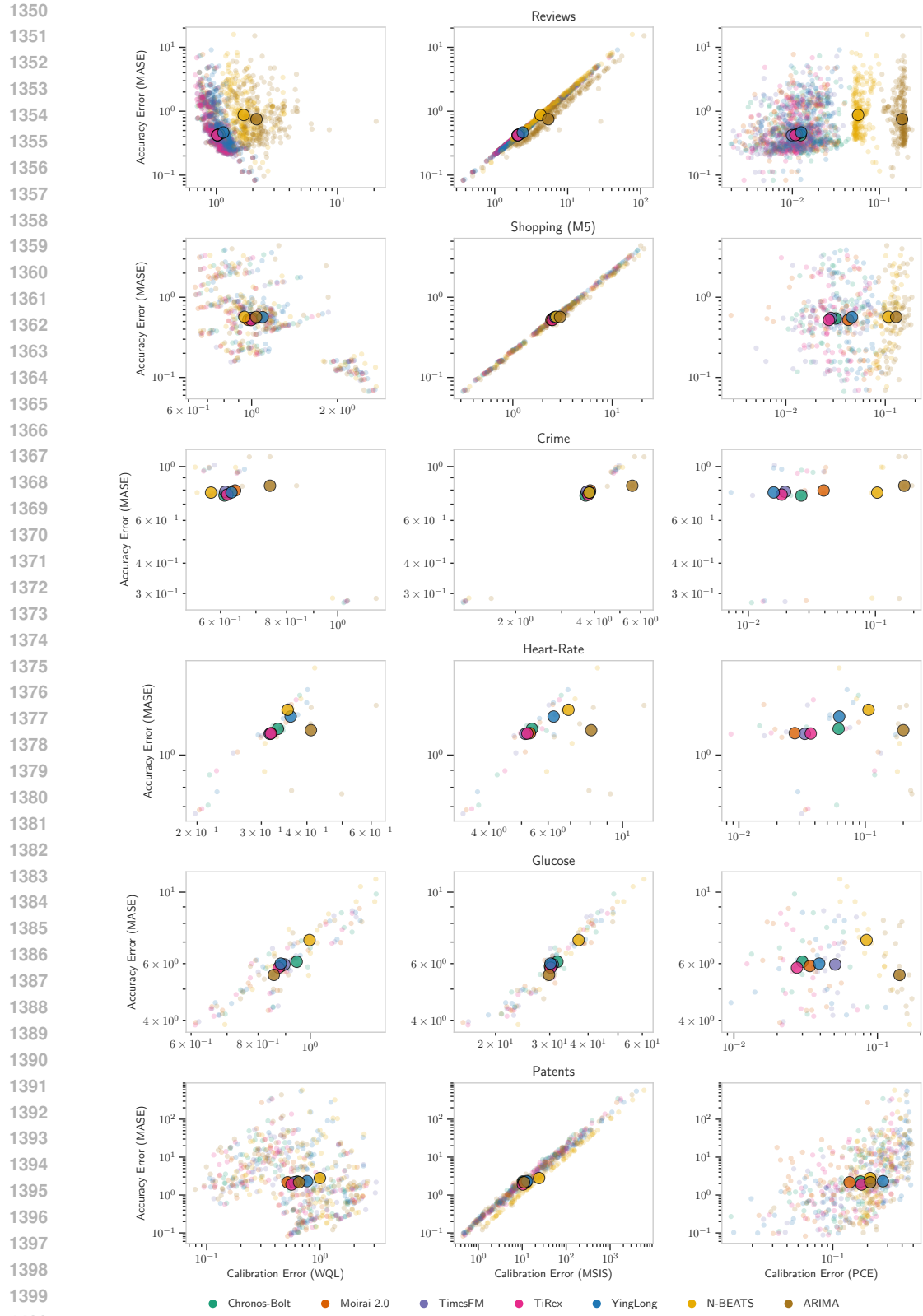


Figure 13: **WQL and MSIS incorrectly imply that N-BEATS and ARIMA are well calibrated on some datasets, while PCE indicates they are always poorly calibrated.** Top: Probabilistic Calibration Error (PCE) across datasets and models using the default quantile prediction head, Patents PCE uses the right y -axis scale. Upper Middle: Weighted Quantile Loss (WQL) measuring a combination of sharpness and calibration. Lower Middle: Mean Scaled Interval Score (MSIS) where Glucose and Patents use right y -axis scale. Bottom: Mean Absolute Scaled Error (MASE) measuring point accuracy of median prediction, Glucose and Patents use the right y -axis scale.

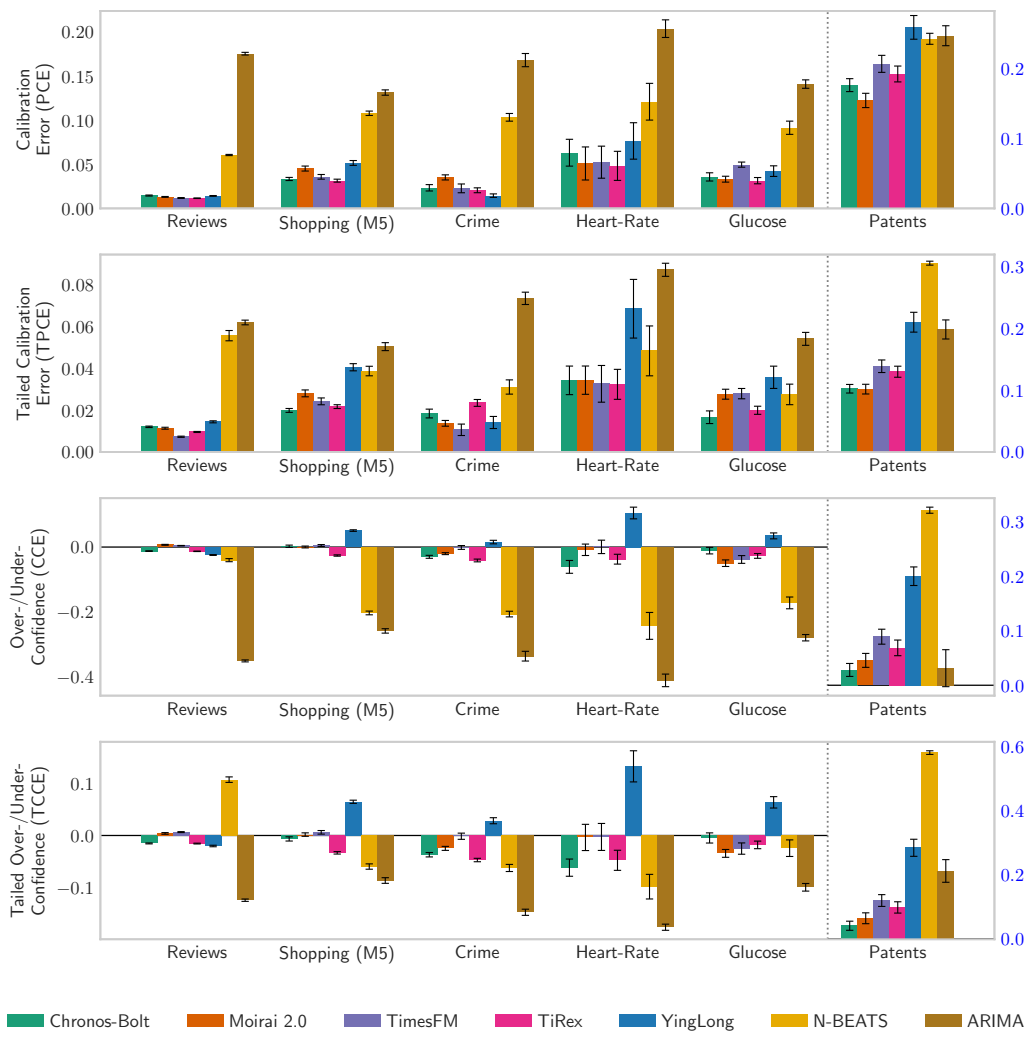


1402
1403

Figure 14: WQL and MSIS are often highly correlated with MASE across time series within a dataset WQL (left), MSIS (middle), and PCE (right) compared to MASE where each dot is the performance of an individual time series.

1404 B.3 TAIL FORECASTING
1405

1406 In downstream tasks such as Anomaly Detection, calibration at the tail ends of probabilistic predictions is more important than at the body of a predictive distribution. We evaluate the tailed calibration with a modified PCE and CCE that only considers the 0.1 and 0.9 quantile predictions rather than averaging over all the quantiles or confidence intervals. The Tailed PCE (TPCE) and Tailed CCE (TCCE) values are not directly comparable to their aggregate values as their scales could be slightly offset. Models that are in general overconfident with positive CCEs tend to be have an exaggerated overconfidence and miscalibration at the tails. The opposite is true with under-confident models, having improved calibration at the tails while their under-confidence CCE is capped and reduced by being at the tail. In Figure 15, we find that YingLong which is overconfident with overly tight confidence intervals, are relatively poorer at the tails of the distribution compared to the other models, while ARIMA sees a relative improvement. For the TSFM models that are neither over nor under-confident, their calibration looks to be improved with very minor calibration error. Promising future work should evaluate tailed calibration with quantiles further on the tail than 0.1 or 0.9 such as 0.001 or 0.999.



1454 **Figure 15: Tailed Calibration Error (TPCE) is generally smaller than Calibration Error (PCE)**
1455 **while Tailed Over-/Under-Confidence (TCCE) grows for overconfident models and reduces for**
1456 **under-confident models.** Comparison of model calibration on the entire probabilistic distribution
1457 versus calibration of the tail-ends of the distribution (0.1 and 0.9).

1458
1459

B.4 ADDITIONAL FINDINGS FOR AR FORECASTING

1460
1461
1462

In this section, we elaborate on two key issues that arise when using short horizons in autoregressive time series forecasting models (TSFMs). Compounding errors degrade accuracy, and block-wise independence introduces bias in the input for future predictions.

1463
1464
1465
1466
1467

1. Autoregressive errors compound. When forecasting multiple time points autoregressively, each predicted value is fed back as input for predicting subsequent points. Even small errors in early predictions can accumulate over the horizon, leading to progressively degraded forecasts.
2. Independent block modeling introduces bias. TSFMs model a block of L future time points as independent given past context:

1470
1471
1472

$$p(x_i, \dots, x_{i+L-1} | x_{<i}) \approx \prod_{j=i}^{i+L-1} p(x_j | x_{<i}).$$

1473
1474
1475
1476
1477
1478
1479

While convenient for training, this ignores any intra-block dependencies. During autoregressive rollouts, the next block of predictions is conditioned on samples from the previous block. Because the sampled block does not preserve the true joint dependencies, the model sees a biased context, resulting in a shift in the marginal distribution of later time points. This bias is larger for longer blocks L (since then there are fewer biased inputs) and vanishes as $L \rightarrow 1$ (where each time point is predicted independently in an autoregressive manner).

1480

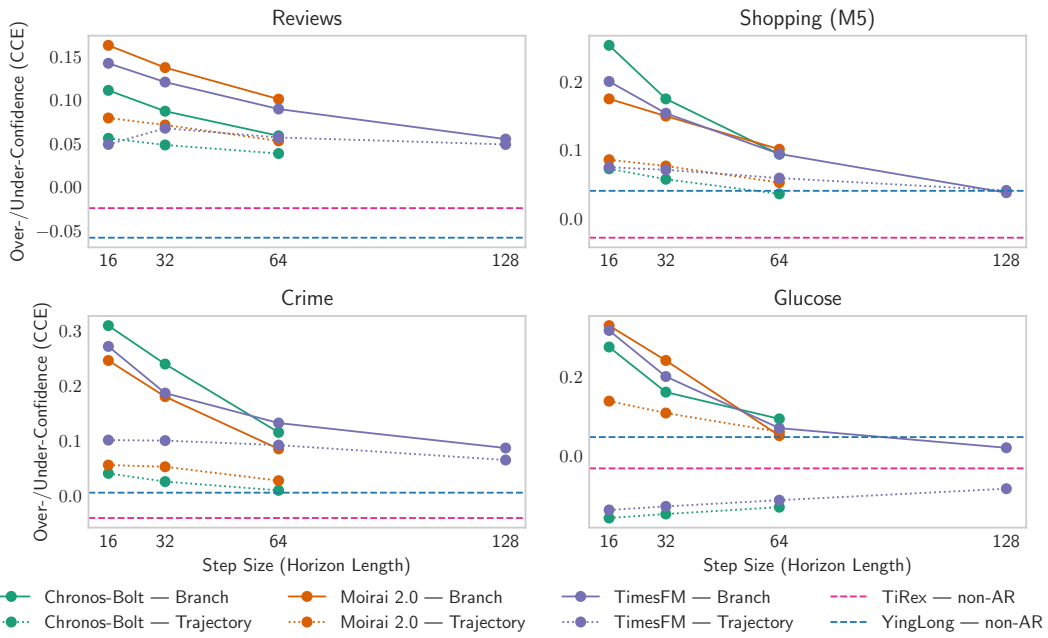
1499
1500
1501

Figure 16: **TSFMs are consistently overconfident on long-term forecasting. The magnitude of the over confidence decreases with longer horizon lengths and when using the trajectory AR method.** The figure compares Centered Calibration Error (CCE) for long-term forecasting using autoregression on the y -axis with AR prediction horizon on the x -axis. The color of the line depicts the model used and the line style indicates the AR method. The pink and blue dashed horizontal lines are the CCE for TiRex and Yinglong without using AR.

1508
1509
1510
1511